



**HAL**  
open science

# Under phosphate starvation conditions, Fe and Al trigger accumulation of the transcription factor STOP1 in the nucleus of Arabidopsis root cells

Christian Godon, Caroline Mercier, Xiaoyue Wang, Pascale David, Pierre Richaud, Laurent Nussaume, Dong Liu, Thierry Desnos

## ► To cite this version:

Christian Godon, Caroline Mercier, Xiaoyue Wang, Pascale David, Pierre Richaud, et al.. Under phosphate starvation conditions, Fe and Al trigger accumulation of the transcription factor STOP1 in the nucleus of Arabidopsis root cells. *Plant Journal*, 2019, 99 (5), pp.937-949. 10.1111/tpj.14374 . cea-02149165

**HAL Id: cea-02149165**

**<https://cea.hal.science/cea-02149165>**

Submitted on 24 Jun 2019

**HAL** is a multi-disciplinary open access archive for the deposit and dissemination of scientific research documents, whether they are published or not. The documents may come from teaching and research institutions in France or abroad, or from public or private research centers.

L'archive ouverte pluridisciplinaire **HAL**, est destinée au dépôt et à la diffusion de documents scientifiques de niveau recherche, publiés ou non, émanant des établissements d'enseignement et de recherche français ou étrangers, des laboratoires publics ou privés.

# *the plant journal*

**Under phosphate starvation condition, Fe and Al trigger the transcription factor STOP1 to accumulate in the nucleus of Arabidopsis root cells.**

Journal:	<i>The Plant Journal</i>
Manuscript ID	TPJ-01389-2018.R1
Manuscript Type:	Original Article
Key Words:	phosphate, iron, aluminum, root, STOP1, ALMT1, Arabidopsis, ALS3

SCHOLARONE™  
Manuscripts

## Running head

Fe and Al trigger nuclear accumulation of STOP1

### Under phosphate starvation condition, Fe and Al trigger the transcription factor STOP1 to accumulate in the nucleus of Arabidopsis root cells

Christian Godon<sup>1\*</sup>, Caroline Mercier<sup>1\*</sup>, Xiaoyue Wang<sup>2</sup>, Pascale David<sup>1</sup>, Pierre Richaud<sup>3</sup>, Laurent Nussaume<sup>1</sup>, Dong Liu<sup>2,4</sup>, Thierry Desnos<sup>1,4</sup>

<sup>1</sup> Laboratoire de Biologie du Développement des Plantes, Commissariat à l'Energie Atomique et aux énergies alternatives, UMR7265 (CEA, Aix-Marseille Université, CNRS), Saint Paul-Lez-Durance F-13108, France.

<sup>2</sup> Ministry of Education Key Laboratory of Bioinformatics, Center for Plant Biology, School of Life Sciences, Tsinghua University, Beijing 100084, China

<sup>3</sup> Laboratoire de Bioénergétique et Biotechnologie des Bactéries et Microalgues, Commissariat à l'Energie Atomique et aux énergies alternatives, UMR7265 (CEA, Aix-Marseille Université, CNRS), Saint Paul-Lez-Durance F-13108, France.

\* These authors contributed equally to this work.

<sup>4</sup> Authors for correspondence.

## Abstract

Low-phosphate (Pi) condition is known to repress the primary root growth of Arabidopsis, in a low-pH and Fe-dependent manner. This growth arrest requires the accumulation of STOP1 transcription factor in the nucleus where it activates the transcription of the malate transporter gene *ALMT1*; exuded malate is suspected to interact with extracellular iron to inhibit root growth. In addition, ALS3 –an ABC-like transporter first identified for its role for tolerance to toxic aluminum– represses nuclear accumulation of STOP1 and the expression of *ALMT1*.

Until now, it was unclear whether phosphate deficiency itself or iron activates STOP1 to accumulate in the nucleus.

Here, by using different growth media to dissociate the effects of Fe from Pi deficiency itself, we demonstrate that Fe is sufficient to trigger the accumulation of STOP1 in the nucleus, which in turn, activates the expression of *ALMT1*. We also show that a low pH is necessary to stimulate the Fe-dependent accumulation of nuclear STOP1. Furthermore, pharmacological experiments indicate that Fe inhibits proteasomal degradation of STOP1. We also show that Al acts like Fe for nuclear STOP1 accumulation and *ALMT1* expression, and that the overaccumulation of STOP1 in the nucleus of the *als3* mutant grown in low-Pi could be abolished by Fe deficiency. Altogether, our results indicate that, under low-Pi condition, Fe<sup>2/3+</sup> and Al<sup>3+</sup> act similarly to increase the stability of STOP1 and its accumulation in the nucleus where it activates the expression of *ALMT1*.

## Significance Statement

Low-phosphate, low-pH and excess aluminum are three major stresses inhibiting root growth. The Arabidopsis transcription factor STOP1 has a major role in root growth

1  
2  
3 51 under these different stresses, but how STOP1 is regulated is not known. Here we  
4 52 show that Fe –instead of low-phosphate– and Al promote the accumulation of  
5 53 STOP1 in root nuclei, in a low-pH-dependent manner. This work unveils an important  
6 54 regulatory step in the response to Al and Fe stresses.  
7 55

### 8 56 **Keywords**

9 57 STOP1, ALMT1, ALS3, phosphate, iron, aluminum, pH, root, nucleus, Arabidopsis.  
10 58

## 11 59 **Introduction**

12 60 In many plant species, Pi-deficiency (-Pi) alters root growth and architecture  
13 61 promoting top-soil foraging: the growth of the primary root is reduced whereas lateral  
14 62 root emergence and growth is stimulated toward a more horizontal direction.  
15 63 Combined, these responses result in root systems that explore relatively better the  
16 64 upper soil horizons where Pi is more concentrated (Lynch, 2001).

17 65 The Arabidopsis primary root stops growing when its apex encounters the -Pi  
18 66 substratum (Svistoonoff et al., 2007). Split-root and feeding experiments showed that  
19 67 this root growth inhibition does not correlate with Pi accumulated inside the root  
20 68 (Thibaud et al., 2010). Instead, it depends of the Pi concentration in the growth  
21 69 medium. This phenomenon was described as the so-called –Pi local response, by  
22 70 opposition to the -Pi systemic responses that are governed by Pi concentration  
23 71 present inside the plant tissues (Puga et al., 2017). While the -Pi systemic response  
24 72 is mainly controlled by the two master regulatory genes *PHOSPHATE STARVATION*  
25 73 *RESPONSE 1 (PHR1)* and *PHR1-like 1 (PHL1)*, the -Pi local response is not  
26 74 (Balzergue et al., 2017). This local growth inhibition response critically depends of  
27 75 the Fe-content of the growth medium (Svistoonoff et al., 2007, Ward et al., 2008,  
28 76 Muller et al., 2015), and iron accumulates in the root tip (Muller et al., 2015,  
29 77 Balzergue et al., 2017, Mora-Macias et al., 2017).

30 78 Inherent to its chemical properties, Pi can form complexes with metallic cations such  
31 79 as  $Fe^{2/3+}$  and  $Al^{3+}$  (Hinsinger, 2001). This has important consequences for the  
32 80 mobility and bioavailability in soil of Pi, Fe and Al as well as for their homeostasis in  
33 81 plants (Hirsch et al., 2006, Misson et al., 2005, Briat et al., 2015, Bouain et al., 2014).  
34 82 In the medium, reflecting the antagonistic Fe-Pi interactions, the Pi/Fe ratio is  
35 83 important: the lower the ratio the higher the inhibition, and when the nutrient solution  
36 84 lacks Fe, the root growth is no more inhibited (Ward et al., 2008, Muller et al., 2015,  
37 85 Svistoonoff et al., 2007).

38 86 During the last decade, major advances contributed to a better understanding of the  
39 87 cellular events underlying the “local” response in Arabidopsis. When exposed to low  
40 88 external Pi (i.e. a low Pi/Fe ratio), the short primary root results from a combination of  
41 89 rapid as well as long-term cellular responses at the root tip. Few hours, if not  
42 90 minutes, after the root tip encounters a Pi-depleted zone, cell elongation decreases.  
43 91 This is correlated with the deposition of iron and accumulation of reactive oxygen  
44 92 species (ROS) in the cell wall of the stem cell niche (SCN) and the elongation zone  
45 93 (EZ), and with a peroxidase-dependent stiffening of the cell wall of the EZ.

46 94 In the long term (hours to days), callose accumulates in cell wall of the root apical  
47 95 meristem (RAM) and EZ, this occludes plasmodesmata and restricts cell-to-cell  
48 96 trafficking. Progressively, root cell proliferation ceases until the exhaustion of the  
49 97 RAM by the on-going cell differentiation (Balzergue et al., 2017, Muller et al., 2015,  
50 98 Mora-Macias et al., 2017).  
51 99  
52 60



1  
2  
3 100 Genetics and molecular analysis identified several proteins governing the root growth  
4 101 inhibition under -Pi. Identified as a major quantitative trait locus, LOW PHOSPHATE  
5 102 ROOT 1 (LPR1) codes a cell wall multicopper oxidase with ferroxidase activity  
6 103 (Svistoonoff et al., 2007, Ticconi et al., 2009, Muller et al., 2015, Reymond et al.,  
7 104 2006). LPR1 has a critical role in the growth arrest because loss-of-function  
8 105 mutations in *lpr1* desensitize the root to -Pi. In particular, they accumulate reduced  
9 106 amount of Fe in their root tip. Upon extended Pi-deprivation, the LPR1-dependent Fe  
10 107 accumulation promotes RAM exhaustion and differentiation by the down-regulation of  
11 108 the root patterning transcription factors SHORT ROOT (SHR) and SCARECROW  
12 109 (SCR). This regulation operates via increased expression of CLAVATA 4 (CLV4), a  
13 110 secreted peptide detected by the plasma membrane receptors CLV2 and  
14 111 CLV2/PEP1 RECEPTOR 2 (PEPR2) (Gutiérrez-Alanís et al., 2017). A higher level of  
15 112 regulation coupling LPR1 with brassinosteroid (BR) signalling pathways has been  
16 113 recently unveiled. In particular, the root growth of seedlings with the constitutively  
17 114 active *bzr1-D* mutation (*BZR1* for *BRASSINAZOLE RESISTANT1*) are unrepressed  
18 115 in -Pi and has reduced expression of *LPR1* (Singh et al., 2014, Singh et al., 2018). In  
19 116 addition, in the wild type (WT), Fe enhances the accumulation of the BR-signalling  
20 117 inhibitor BKI1 (BRASSINOSTEROID KINASE INHIBITOR1), thereby closing a  
21 118 feedback regulatory loop between LPR1 activity and BR signalling.  
22 119 *PHOSPHATE DEFICIENCY RESPONSE 2* (*PDR2*) was the first gene identified in  
23 120 the local response (Ticconi et al., 2004). *PDR2* is the only Arabidopsis P5-type  
24 121 ATPase; it is located in the endoplasmic reticulum and its substrate is not yet known  
25 122 (Ticconi et al., 2009). Compared to *lpr1* mutations, a mutation inactivating *PDR2*  
26 123 confers an opposite effect (i.e. over accumulation of Fe) (Muller et al., 2015). The  
27 124 *lpr1* mutations are epistatic over *pdr2* indicating a functional interaction between  
28 125 LPR1 and PDR2.  
29 126

30 127 A large-scale forward genetics screen for seedlings with a primary root less sensitive  
31 128 to -Pi inhibition identified several *stop1* and *almt1* mutants (in addition to *lpr1*)  
32 129 (Balzergue et al., 2017). *STOP1* (SENSITIVE TO PROTON RHIZOTOXICITY1) is a  
33 130 C<sub>2</sub>H<sub>2</sub> zinc finger transcription factor necessary for the expression of *ALUMINUM*  
34 131 *ACTIVATED MALATE TRANSPORTER 1* (*ALMT1*), coding a plasma membrane  
35 132 transporter exuding malate (Hoekenga et al., 2006, Iuchi et al., 2007). While the  
36 133 *stop1* and *almt1* mutants have reduced accumulation of Fe in the EZ, they still  
37 134 accumulate large amount of Fe in the stem cell niche (SCN) (Balzergue et al., 2017,  
38 135 Wang et al., 2019), although others observed reduced accumulation of Fe in SCN  
39 136 (Mora-Macias et al., 2017). This is correlated with some remaining root inhibition  
40 137 upon long-term -Pi deprivation, presumably mediated by the Fe-dependent RAM  
41 138 differentiation and exhaustion. These observations show that the STOP1-ALMT1  
42 139 module is mainly involved in the inhibition of cell elongation whereas the LPR1-PDR2  
43 140 module influences all aspects of the local response. Supporting independent genetic  
44 141 regulations of these two modules, the *lpr1* mutation does not alter the expression of  
45 142 *ALMT1* and, reciprocally, *stop1* mutants display WT expression of *LPR1*. It seems  
46 143 that, at least in the elongation zone, the convergence point of these two modules is in  
47 144 the apoplast compartment where the ALMT1-exuded malate somehow helps the Fe  
48 145 to participate in the generation of ROS.  
49 146

50 147 In the root tip, Pi deprivation enhances the transcript level of *ALMT1* but not of  
51 148 *STOP1*, suggesting a post-translational regulation of STOP1 protein. Indeed, the -Pi  
52 149 condition stimulates the accumulation of STOP1 in the nucleus (Balzergue et al.,

1  
2  
3 150 2017). This nuclear accumulation of STOP1 represents therefore an important  
4 151 control step in this pathway for which a first, and unexpected, regulatory component  
5 152 has been identified recently. A genetics screen for mutants hypersensitive to -Pi  
6 153 induced root growth inhibition retrieved an *als3* mutant. The ALS3 protein  
7 154 (ALUMINUM SENSITIVE 3) interacts with STAR1 (SENSITIVE TO ALUMINUM  
8 155 RHIZOTOXICITY 1) to form a putative ATP-binding cassette (ABC) transporter  
9 156 complex located in the tonoplast (Dong et al., 2017). Consistently, in -Pi, the *star1*  
10 157 mutant behaves like *als3*. Interestingly, the root hypersensitivity of *als3* and *star1*  
11 158 correlates with higher accumulation of STOP1 in root nuclei and overexpression of  
12 159 *ALMT1* in the root tip. By contrast, in -Pi, the overexpression of the ALS3-STAR1  
13 160 fusion protein represses the accumulation of STOP1 in the nucleus and improves  
14 161 root growth of WT. Moreover, a suppressor screen of *als3* identified *stop1* and *almt1*  
15 162 mutants (as well as *lpr1*) (Wang et al., 2019). Taken together, these results show  
16 163 that, in combination, ALS3 and STAR1 attenuate the root growth inhibition in -Pi by  
17 164 repressing the accumulation of STOP1 in the nucleus. This led us to hypothesize that  
18 165 ALS3-STAR1 depletes an unknown cytosolic compound (toward the vacuole) that  
19 166 enhances the accumulation of STOP1 in the nucleus (Wang et al., 2019).  
20  
21  
22  
23

24 168 Before the discovery of their implication in the response to -Pi, STOP1, ALMT1,  
25 169 ALS3 and STAR1 were all known for their major role in Arabidopsis resistance  
26 170 against toxic aluminum. Loss-of-function mutations in any of these genes severely  
27 171 impair root growth in the presence of Al<sup>3+</sup> (Larsen et al., 2005, Iuchi et al., 2007,  
28 172 Huang et al., 2010, Hoekenga et al., 2006). It is therefore tempting to deduce that in  
29 173 Pi deprived conditions, Fe<sup>2/3+</sup> is the responsible metallic ion triggering nuclear  
30 174 accumulation of STOP1, thereby participating to root growth repression in -Pi.  
31  
32

33 176 In this work, we found growth conditions with limited Pi allowing to distinguish the  
34 177 effect of Fe from the -Pi *per se*. This enabled us to compare the effect of Fe with Al  
35 178 on STOP1 and ALMT1. Our results demonstrate that Fe, as well as Al, triggers the  
36 179 accumulation of STOP1 in the nucleus and the expression of *ALMT1*.  
37  
38

## 39 181 Results

40 182 We previously showed that the low-Pi condition stimulates the expression of the  
41 183 *ALMT1* gene, and this stimulation relies on the transcription factor STOP1 (Balzergue  
42 184 et al., 2017). In addition, under low-Pi, omitting Fe in the nutrient solution prevents  
43 185 the root growth arrest, showing that Fe is essential for this growth response  
44 186 (Svistoonoff et al., 2007, Ward et al., 2008, Dong et al., 2017, Muller et al., 2015,  
45 187 Mora-Macias et al., 2017). However, the -Fe conditions previously tested did not  
46 188 completely suppress the expression of *ALMT1*.  
47  
48

### 49 190 Fe, but not Pi deficiency *per se*, induces *ALMT1* expression

50 191 We used the *pALMT1::GUS* (GUS, β-glucuronidase) construct to investigate the role  
51 192 of Fe because this visual reporter sensitively allows to test the activity of the STOP1  
52 193 signalling in the root tip (Balzergue et al. 2017). We first tested the influence of the  
53 194 Pi/Fe ratio on the expression of *ALMT1*. Seedlings were first grown 3 days on a -Pi  
54 195 medium without Fe added. To prevent the expression of *ALMT1* (and thus the  
55 196 accumulation of the GUS protein) during this pre-culture, the growth medium was  
56 197 buffered at pH 6.7. Indeed, at pH around neutrality we observed no or very little GUS  
57 198 staining in the root tip of *pALMT1::GUS* seedlings (Balzergue et al. 2017 & Figure  
58 199 S1). Seedlings were then transferred from this pre-culture condition, to media

1  
2  
3 200 differing by their Fe to Pi ratio, at pH 5.5. Twenty-four hours after transfer, the  
4 201 seedlings were stained for GUS activity. In a medium supplemented with 15  $\mu\text{M}$  of  
5 202 Fe, and without Pi added, there is a strong expression of *ALMT1* (Figure 1a).  
6 203 Increasing the Pi content reduces the expression of *ALMT1*. However, at the highest  
7 204 Pi concentration tested (250  $\mu\text{M}$ ), the expression of *ALMT1* is still induced. This  
8 205 result confirms that *ALMT1* expression is higher in -Pi compared to +Pi condition.  
9 206 However, increasing the Fe content in a medium containing 250  $\mu\text{M}$  Pi, increases the  
10 207 expression of *ALMT1* (Figure 1b). This confirms result of Müller et al (2015) and  
11 208 suggests that Fe, instead of Pi deficiency *per se*, stimulates the expression of  
12 209 *ALMT1*.

13 210 We observed that even without supplementing the -Pi growth medium with Fe, at pH  
14 211 5.5, there was still a strong expression of *ALMT1* (Figure 2a, first picture). It  
15 212 prompted us to assay putative presence of iron in the agar using a quantification by  
16 213 ICP-AES (Inductively Coupled Plasma – Absorption Emission Spectrometry). This  
17 214 analysis revealed the presence of 38  $\mu\text{g Fe}\cdot\text{g}^{-1}$  agar (5.5  $\mu\text{M}$  Fe in the final growth  
18 215 medium) (Table S1).

19 216 To further test the hypothesis that, in -Pi condition, the Fe that was contained in the  
20 217 agar powder is the trigger of *ALMT1* expression, we reduced the availability of Fe in  
21 218 the growth media using a siderophore. Supplementing the medium with 100  $\mu\text{M}$   
22 219 deferoxamine (DFO), a potent Fe-chelator, strongly diminished *ALMT1* expression,  
23 220 (Figure 2a). DFO was effective in chelating Fe since addition of 15  $\mu\text{M}$  Fe did not  
24 221 stimulate expression of *ALMT1* (Figure 2a). To avoid the potential toxicity of a high  
25 222 concentration of DFO that could interfere with gene expression, an alternative  
26 223 approach was used to reduce bioavailable iron from the agar. The agar powder was  
27 224 mixed with DFO and then washed (see Experimental procedures). We then tested  
28 225 whether the level of expression of *ALMT1* remained low. In -Pi plates made with this  
29 226 washed, DFO-treated agar, the expression of *ALMT1* is almost fully abolished, and  
30 227 addition of 15  $\mu\text{M}$  Fe restored a high level of expression (Figure 2b). We conclude  
31 228 that a strong chelator of Fe suppresses the expression of *ALMT1*. Altogether, these  
32 229 results show that the stimulation of *ALMT1* expression in -Pi condition is triggered by  
33 230 Fe but not by the Pi-deficiency *per se*.

34 231  
35 232 This result prompted us to compare the expression of *ALMT1* with that of *SPX1*  
36 233 (*SYG1/Pho81/XPR1*), a classical marker of the -Pi stress. *SPX1* encodes a protein  
37 234 regulating the activity of the transcription factor *PHR1* –a master regulator of the -Pi  
38 235 stress, and is frequently used as a marker of the -Pi transcriptional response. To  
39 236 monitor its expression, we used WT seedlings containing the *pSPX1::GUS* marker  
40 237 (Duan et al., 2008). The *pALMT1::GUS* and *pSPX1::GUS* seedlings were grown in +  
41 238 or -Pi, at pH 5.5 or 6.7, and with two different agars or an agarose; in all these media  
42 239 the nutrient solution was not supplemented with Fe.

43 240 As already shown (Balzergue et al., 2017), on an agar containing Fe, the expression  
44 241 of *ALMT1* is induced at pH 5.5 but not at pH 6.7, in both -Pi and +Pi (Figure 3a). This  
45 242 expression is much less stimulated in media that contain very low amount of Fe  
46 243 (DFO-treated agar or on the agarose Seakem, Figure 3a and Supplementary Table  
47 244 1). By contrast, the expression of *SPX1* is induced only in -Pi conditions, whatever  
48 245 the pH or the gelifying agent used to prepare the growth medium (Figure 3a). All  
49 246 these observations were confirmed by qRT-PCR (Quantitative Reverse  
50 247 Transcriptase-Polymerase Chain Reaction) (Figure 3b and Figure S2), and with the  
51 248 *PPsPase1* (pyrophosphatase [PPi]-specific phosphatase1) gene as an additional  
52 249

1  
2  
3 249 marker whose expression is highly stimulated by Pi-deficiency (Hanchi et al., 2018)  
4 250 (Figure 3b).

5 251 We also monitored the expression of the *IRT1* (IRON-REGULATED  
6 252 TRANSPORTER 1) gene, a well-known indicator of Fe deficiency (Vert et al., 2002).  
7 253 This marker indicates that, as expected, when grown on the Sigma-DFO agar plates,  
8 254 seedlings are more Fe starved than on the other plates (Figure 3b). On plates made  
9 255 with the Seakem agar, that contains very low amount of Fe, *IRT1* is also more  
10 256 expressed than with the Sigma agar (Figure 3b). These analyses of genes  
11 257 expression further show that *ALMT1* is not stimulated by the -Pi *per se*, and strongly  
12 258 suggest that the signal stimulating the expression of *ALMT1* is distinct from that of  
13 259 the SPX1 pathway. By contrast to *ALMT1* mRNA, Al, Fe and pH do not modulate the  
14 260 level of *STOP1* mRNA accumulation (Figure S3).  
15 261

### 18 262 **Fe stimulates STOP1 accumulation in the nucleus**

19 263 With the *pSTOP1::GFP-STOP1* reporter, we previously showed that STOP1  
20 264 accumulates in the nuclei at the primary root tip seedlings grown in -Pi (Balzergue et  
21 265 al., 2017, Wang et al., 2019). Our gene expression analysis of *ALMT1* incited us to  
22 266 test whether Fe is involved in this nuclear accumulation of STOP1.

23 267 Seedlings carrying the *pSTOP1::GFP-STOP1* marker were grown 3 days in non-  
24 268 inducible conditions (i.e. agarose Seakem without addition of Pi and Fe that do not  
25 269 stimulate the expression of *ALMT1*, as shown in Figure 3a), transferred in the same  
26 270 medium supplemented or not with Fe before examining the GFP-fluorescence. We  
27 271 first assessed the range of Fe concentrations that stimulate nuclear accumulation of  
28 272 STOP1 in acidic condition (pH 5.5). Figure 4a (and Figure S4a for an independent  
29 273 experiment) shows that from 0 to 60  $\mu$ M Fe GFP-fluorescence in the nuclei increases  
30 274 with Fe concentration; a plateau is reached around 60  $\mu$ M Fe. Note that without Fe,  
31 275 we observe small fluorescent dots in cells (first picture in Figure 4a). These dots are  
32 276 autofluorescence of root cell components (i.e. not GFP fluorescence) since a WT  
33 277 seedling that does not carry the GFP marker displays similar dots (Figure S5).

34 278 Since in non-inducible conditions we do not detect GFP fluorescence in the  
35 279 cytoplasm, we hypothesized that the accumulation of GFP-STOP1 protein in the  
36 280 nucleus results from reduced proteasomal degradation (instead of i.e. translocation  
37 281 form cytosol). We then tested the effect of MG132, an inhibitor of the 26S  
38 282 proteasome, on the accumulation of GFP-STOP1 in seedlings grown in a moderate  
39 283 amount of Fe (Agar Sigma without addition of Fe, see Table S1). When treated with  
40 284 MG132, the GFP fluorescence substantially accumulated in the nucleus (Figure 4b,  
41 285 see also Figure S6 for additional pictures of two independent experiments). This  
42 286 result therefore supports the idea that Fe somehow inhibits the degradation of  
43 287 STOP1 by the 26S proteasome.  
44 288

45 289 We then performed a kinetic analysis, at pH 5.5, of the nuclear accumulation of  
46 290 STOP1. Figure 4c (and Figure S4b) shows that in seedlings transferred in a medium  
47 291 without Fe added (-Fe), the level of nuclear GFP-fluorescence remains low through  
48 292 the 3 h of the kinetic. By contrast, after transfer of seedlings onto plates containing 60  
49 293  $\mu$ M Fe, the GFP fluorescence in nuclei increases after 30 min and becomes higher  
50 294 than in the -Fe control after 1h; and the fluorescence further increases with time. This  
51 295 confocal analysis, performed in -Pi condition for all conditions, indicates that Fe, and  
52 296 not the -Pi condition *per se*, rapidly promotes the accumulation of STOP1 in the  
53 297 nucleus.  
54 298  
55 299  
56 300  
57  
58  
59  
60



1  
2  
3 298 We have shown previously that the acidity of the growth medium is a crucial  
4 299 parameter to stimulate *ALMT1* expression (Balzergue et al., 2017). We therefore  
5 300 tested whether low pH on its own also promotes the nuclear accumulation of STOP1.  
6 301 Figure 4d (and Figure S4c) shows that, indeed, in presence of 60  $\mu\text{M}$  Fe, the level of  
7 302 nuclear GFP-fluorescence of GFP-STOP1 is higher in acidic conditions, whereas at  
8 303 pH 6.7 it is low and does not significantly differ from the -Fe control. This confirms the  
9 304 result shown in Figure 4a: an acidic pH (below 6.1) without Fe does not stimulate  
10 305 accumulation of GFP-STOP1 in the nucleus. These measures show that a low pH is  
11 306 required, but not sufficient, to stimulate nuclear accumulation of STOP1; the  
12 307 accumulation occurs only in acidic conditions supplemented with Fe. This comforts  
13 308 results shown in Figure 3 about the expression of *ALMT1*.  
14 309

### 17 310 **Aluminum triggers STOP1 accumulation in the nucleus**

18 311 STOP1 and *ALMT1* participate to resistance against  $\text{Al}^{3+}$  toxicity, and  $\text{Al}^{3+}$  stimulates  
19 312 the expression of *ALMT1*. As, for Fe (Figure 2b), in seedlings grown on plates made  
20 313 with the washed, DFO-treated agar, the expression of *ALMT1* is restored by addition  
21 314 of 15  $\mu\text{M}$   $\text{Al}^{3+}$  (Figure S7). We therefore asked whether  $\text{Al}^{3+}$  also stimulates STOP1 to  
22 315 accumulate in the nucleus. Seedlings were grown 3 days in agarose Seakem plates,  
23 316 and transferred for 2 h in plates supplemented or not with  $\text{Al}^{3+}$  before observing GFP-  
24 317 fluorescence of GFP-STOP1. Preliminary observations showed GFP-fluorescence in  
25 318 the nucleus after the transfer in Al-plates. A dose-response curve indicated that 15  
26 319  $\mu\text{M}$   $\text{Al}^{3+}$  is sufficient to detect an accumulation of GFP in the nucleus, and a plateau is  
27 320 reached at about 30  $\mu\text{M}$   $\text{Al}^{3+}$  (Figure 5a and Figure S8a for an independent  
28 321 experiment). A kinetic indicates that 1 h after transfer the GFP signal is already  
29 322 significantly higher than the control not supplemented with Al (Figure 5b, Figure S8b).  
30 323 The signal further increases through the 3 h kinetic.

31 324 As for Fe, a low-pH (from 5.5 to 6.7) is required to Al to promote the nuclear  
32 325 accumulation of the GFP-STOP1 (Figure 5c and Figure S8c). These experiments  
33 326 show that Al, as Fe, rapidly triggers nuclear accumulation of STOP1 when the growth  
34 327 conditions are acidic.  
35 328

### 39 329 **The overaccumulation of STOP1 in root nuclei of *als3* is Fe-dependent**

40 330 Using the *pSTOP1::GFP-STOP1* marker we previously shown that in the *als3* and  
41 331 *star1* mutants, the accumulation of GFP-STOP1 in root nuclei is much higher than in  
42 332 the WT (Wang et al., 2019). We thus asked whether this overaccumulation depends  
43 333 of Fe. We confirmed that, when grown on agarose Seakem plates supplemented with  
44 334 60  $\mu\text{M}$  Fe, the *als3* mutant accumulates much more GFP-STOP1 in nuclei than the  
45 335 WT control (Figure 6). In -Fe, this accumulation is suppressed in both the WT and the  
46 336 *als3* mutant (Figure 6). This result was confirmed with the DFO-agar (Figure S9).  
47 337 Therefore, the enhanced accumulation of nuclear GFP-STOP1 in *als3* root nuclei  
48 338 depends of Fe. Our results show that Fe is critical for STOP1 to accumulate in  
49 339 nucleus, and ALS3 repress this accumulation in a Fe-dependent manner.  
50 340

## 53 341 **Discussion**

54 342 We, and others, have previously shown that several aspects of the root growth arrest  
55 343 under -Pi conditions are Fe-dependent (Svistoonoff et al., 2007, Ward et al., 2008,  
56 344 Dong et al., 2017, Muller et al., 2015, Gutiérrez-Alanís et al., 2017, Singh et al., 2018,  
57 345 Wang et al., 2019), but the relationships between -Pi and Fe were unclear. Here, we  
58 346 focused our work on the STOP1 signalling and succeed to dissociate the effect of -Pi  
59 347 itself from the role of Fe in the STOP1 signalling.

1  
2  
3 348 We compared the expression of *SPX1* and *PPsPase* genes as marker of the  
4 349 systemic -Pi stress with that of *ALMT1* that belongs to the local -Pi-stress. We show  
5 350 that, in the root, Fe stimulates the expression of *ALMT1* regardless the concentration  
6 351 of Pi, and the -Pi-Fe as well as the +Pi-Fe conditions decrease the expression of  
7 352 *ALMT1*. In addition, we demonstrate that the accumulation of STOP1 in root tip  
8 353 nuclei is Fe-dependent. By contrast, the expression of *SPX1* and *PPsPase* happens  
9 354 only under the -Pi condition and it is not correlated with the availability of Fe in the  
10 355 medium (Figure 3 and Figure S2). Supporting this conclusion, our previous results  
11 356 showed that the expression of *ALMT1* in -Pi does not depend of *PHR1* and *PHL1*  
12 357 genes (Balzergue et al., 2017), two targets of *SPX1* regulation (Puga et al., 2014).  
13 358 We thus demonstrate that, under -Pi conditions, it is the Fe and not the -Pi condition  
14 359 itself that stimulates the accumulation of STOP1 in root nuclei and the transcription of  
15 360 *ALMT1*. Under +Pi, Fe is probably associated with Pi molecules, thus hampering the  
16 361 Fe-dependent regulation of nuclear STOP1 and the catalysis of ROS production,  
17 362 whereas under -Pi condition, Fe is more available to stimulate these two processes.  
18 363 Therefore, the STOP1 signalling pathway is clearly distinct from the systemic -Pi  
19 364 signalling, at least the *PHR1*- and *PHL1*-dependent pathway.  
20  
21  
22  
23

### 24 366 **Fe and Al stimulate the accumulation of STOP1 in the nucleus**

25 367 Our work demonstrates that Fe and  $Al^{3+}$  stimulate the accumulation of STOP1 in the  
26 368 nucleus. In previous works by others, the cellular localisation of Arabidopsis STOP1  
27 369 and STOP1 homologues was assessed by transient expression in onion cells,  
28 370 Arabidopsis protoplasts, protoplasts derived from rice callus, tobacco leaves or  
29 371 *Nicotiana benthamiana* leaves. In all these assays, the STOP1 proteins, fused to the  
30 372 GFP, were localized in the nucleus (Sawaki et al., 2009, Sawaki et al., 2014, Fan et  
31 373 al., 2015, Daspute et al., 2018, Huang et al., 2018, Wang et al., 2017, Wu et al.,  
32 374 2018, Yamaji et al., 2009, Che et al., 2018). In these assays, the growth media used  
33 375 were not phosphate deficient or particularly enriched in Fe or  $Al^{3+}$ . This suggests that,  
34 376 in these experimental conditions, the pathway stimulating or repressing the  
35 377 accumulation of STOP1 in the nucleus is constitutively active or inactive,  
36 378 respectively. Supporting this last idea, an immunostaining experiment showed a  
37 379 constitutive nuclear localization of OsART1 in WT root cells (i.e. not affected by Al  
38 380 treatment) (Yamaji et al., 2009). Another possibility is that overexpression of the  
39 381 STOP1 protein saturates the putative regulatory mechanism governing its nuclear  
40 382 accumulation. Alternatively, these STOP1 proteins are differently regulated in these  
41 383 cells compared to the root cells of Arabidopsis.  
42  
43  
44

45 384  
46 385 In the past, we have shown that under neutral pH condition the root growth is not  
47 386 arrested in low-Pi (Svistoonoff et al., 2007) and *ALMT1* is not expressed (Balzergue  
48 387 et al., 2017). These two phenomena are now explained (at least partially) as we  
49 388 show that under low-pH without Fe or  $Al^{3+}$ , STOP1 does not accumulate in the  
50 389 nucleus and, reciprocally, in the presence of Fe or  $Al^{3+}$ , but at pH 6.7 STOP1 does  
51 390 not accumulate in the nucleus either (Figures 4 and 5). The low pH is thus a  
52 391 necessary but not sufficient condition to stimulate nuclear STOP1.

53 392 Our qRT-PCR result shows that *IRT1* — a gene whose expression is induced when  
54 393 Fe is poorly available, like on the DFO-agar (Figure 3b) — is not or poorly induced at  
55 394 pH 6.7 (Figure 3b, agar Sigma and agarose Seakem), indicating that seedlings are  
56 395 not Fe-deficient. Nevertheless, this pH prevents the accumulation of STOP1 in the  
57 396 nucleus. This suggests that different Fe signalling or different pools or forms of Fe  
58 397 regulate *IRT1* expression and STOP1 nuclear accumulation. Knowing that  $Fe^{2/3+}$  and  
59  
60

1  
2  
3 398  $\text{Al}^{3+}$  are soluble only under low pH, STOP1 regulation seems sensitive to the cationic  
4 399 form of Fe and Al.

5 400  
6 401 The first *stop1* mutant was originally identified for its defective root growth on agar  
7 402 plates made with a MS medium at pH 4.3 (Iuchi et al., 2007). The authors confirmed  
8 403 the hypersensitivity to low-pH by using hydroponic culture; this growth medium  
9 404 contained only submicromolar concentration of Fe (and no Pi). According to the  
10 405 results presented here, under acidic conditions without Fe (or  $\text{Al}^{3+}$ ), STOP1 poorly  
11 406 accumulates in the nucleus. Then, if STOP1 does not accumulate in nucleus under  
12 407 these growth conditions, how does it participate to resistance against low-pH? One  
13 408 hypothesis is that a very low amount of Fe, at pH 4.3, is sufficient to stimulate the  
14 409 accumulation of STOP1 for triggering the expression of genes for  $\text{H}^+$  tolerance.  
15 410 Alternatively, STOP1 might have already started promoting the expression of genes  
16 411 involved in  $\text{H}^+$  tolerance before (i.e. during embryogenesis) seedlings encounter  
17 412 acidic conditions. A transcriptomic study on seedlings grown in acidic environment  
18 413 shown that *stop1* mutant is defective for the expression of several genes, including  
19 414 genes involved in cell wall composition or modelling (Sawaki et al., 2009).  
20 415 Furthermore, physiological studies suggested that *stop1* seedlings are defective in a  
21 416 mechanism alleviating  $\text{H}^+$  toxicity, via perhaps  $\text{Ca}^{2+}$  stabilization of the cell wall  
22 417 (Kobayashi et al., 2013b). It is therefore tempting to speculate that already during WT  
23 418 embryogenesis, STOP1 participates in the making of root cells with a cell wall able to  
24 419 tolerate  $\text{H}^+$  during few days after germination, and in the *stop1* seeds the root cell  
25 420 wall are somehow altered, leading to reduced root growth under acidic conditions.  
26 421

### 27 422 **ALS3 and STAR1 repress the accumulation of STOP1 in the nucleus**

28 423 In a previous work, Wang et al demonstrated that, together, ALS3 and STAR1  
29 424 repress the accumulation of STOP1 in the nucleus (Wang et al., 2019). ALS3 and  
30 425 STAR1 associate to form an ABC-type transporter located in the tonoplast. We thus  
31 426 inferred a model whereby a cytosolic metabolite stimulates the accumulation of  
32 427 STOP1 in the nucleus, and that ALS3-STAR1 transporter pumps this metabolite from  
33 428 the cytosol to the vacuole. According to this model, the cytosolic concentration of this  
34 429 metabolite is higher in *als3* and *star1* mutants than in WT, thereby increasing nuclear  
35 430 STOP1.

36 431 We showed here that the overaccumulation of STOP1 in the nucleus of *als3* mutant  
37 432 is abrogated when the seedling grows in a Fe-depleted medium (Figure 6). Since our  
38 433 results on the nuclear STOP1 with  $\text{Al}^{3+}$  are similar to those with Fe, this metabolite  
39 434 could be the trivalent metal ( $\text{Fe}^{3+}$  or  $\text{Al}^{3+}$ ) or a Fe (or  $\text{Al}^{3+}$ )-containing molecule. This  
40 435 hypothesis would fit with the role of ALS3-STAR1 in  $\text{Al}^{3+}$  tolerance. However, we  
41 436 cannot exclude that this metabolite does not contain Fe (or  $\text{Al}^{3+}$ ).  
42 437

43 438 The *STOP1*, *ALS3* and *STAR1* genes are all expressed in the root tip (Larsen et al.,  
44 439 2005, Dong et al., 2017, Balzergue et al., 2017, Mora-Macias et al., 2017); this is  
45 440 coherent with their role as a shared functional unit.  
46 441

### 47 442 **The two effects of Fe on root growth arrest**

48 443 A two-branched regulatory pathway modulates the root growth arrest: the  
49 444 STOP1/ALMT1/ALS3/STAR1 branch and the LPR1/PDR2 branch (Balzergue et al.,  
50 445 2017, Abel, 2017, Wang et al., 2019). These two branches are converging on the Fe-  
51 446 dependent production of ROS in the cell wall. In the *lpr1* mutant the expression of  
52 447 *ALMT1* is not altered compared to WT (Balzergue et al., 2017). This means that in



1  
2  
3 448 the *lpr1* mutant, STOP1 is as active as in the WT. Since the *lpr1* root tip accumulates  
4 449 far less extracellular Fe and ROS than in the WT, ROS and extracellular Fe seem not  
5 450 crucial for activating STOP1 for *ALMT1* expression. Instead, our present work with  
6 451 ALS3 indicates that an intracellular metabolite (containing Fe or Al<sup>3+</sup>?) activates the  
7 452 STOP1 branch.

8 453 In Figure 7 a model summarizes our current knowledge of this two-branched  
9 454 pathway. The phosphate ions inactivate Fe by forming a complex with it. Under -Pi  
10 455 condition, Fe is released from this complex. Fe –or an unknown compound–  
11 456 accumulates in the cell where it stimulates the accumulation of STOP1 in the nucleus  
12 457 by inhibiting its proteasomal degradation. Inside the nucleus STOP1 activates the  
13 458 transcription of *ALMT1*. The *ALMT1* protein exudes malate in the apoplast where,  
14 459 together with Fe and the ferroxidase LPR1, they generate ROS that inhibit cell wall  
15 460 expansion via the cross-linking activity of cell wall peroxidases. In the tonoplast  
16 461 membrane, ALS3 and STAR1 pump Fe –or the unknown compound– from the  
17 462 cytosol to the vacuole compartment. It follows that the concentration of Fe, or the  
18 463 unknown compound, in the cytosol decreases and this reduces the accumulation of  
19 464 STOP1 in the nucleus, and therefore reduces also the expression of *ALMT1*.

20 465 Note that Fe has two effects: it directly or indirectly activates the accumulation of  
21 466 STOP1 in the nucleus and it also participates to the generation of ROS in the  
22 467 apoplast. These two effects can be uncoupled; for example, the *lpr1* mutant still  
23 468 expresses *ALMT1* but its root growth is not inhibited under -Pi.

24 469 For the aluminium, the model only partially applies because the exuded malate  
25 470 prevents the inhibitory effect of toxic Al<sup>3+</sup> on root growth. In addition, we do not know  
26 471 whether ALS3 and STAR1 pump Al<sup>3+</sup>. In any case, Fe and Al<sup>3+</sup> share several  
27 472 characteristics in the nuclear accumulation of STOP1: dependency to low-pH, similar  
28 473 kinetics, negative role of ALS3-STAR1. This could mean that Fe and Al<sup>3+</sup> have  
29 474 some common signalling steps activating STOP1. Many points remain obscure or not  
30 475 yet demonstrated in this model. In particular, how cellular Fe (and Al<sup>3+</sup>) regulates  
31 476 STOP1.

32 477

### 33 478 **How the Fe and Al stimulate STOP1 accumulation in nucleus?**

34 479 In plants, few Fe-sensing proteins have been identified (Kobayashi & Nishizawa,  
35 480 2012). The HRZ (Haemerythrin motif-containing Really Interesting New Gene  
36 481 (RING)-and Zinc-finger) proteins BRUTUS (BTS), BTS-like, OsHRZ1 and OsHRZ2  
37 482 are E3 ligases involved in the low-Fe response (Kobayashi et al., 2013a, Long et al.,  
38 483 2010, Hindt et al., 2017). They target to proteasomal degradation several basic helix-  
39 484 loop-helix transcription factors like the POPEYE (PYE) and PYE-like such as  
40 485 bHLH104 and bHLH105, which are positive regulators of the low-Fe response. Under  
41 486 Fe-sufficient condition, the binding of Fe to the hemerythrin domains destabilizes the  
42 487 HRZ proteins, thereby relieving the transcriptional response to low-Fe (Selote et al.,  
43 488 2015, Kobayashi et al., 2013a). Also involved in transcriptional regulation of the Fe-  
44 489 homeostasis are the IDEF1 and IDEF2 proteins that bind Fe, as well as zinc  
45 490 (Kobayashi et al., 2012).

46 491 Here we have shown that MG132, an inhibitor of the 26S proteasome, substantially  
47 492 increases the level of GFP-STOP1 accumulated in the nucleus in seedlings grown in  
48 493 poorly inductive conditions (i.e. low-Fe; Figure 4b and Figure S6). This indicates that  
49 494 under poorly or non-inductive conditions, STOP1 is degraded by the 26S-proteasome  
50 495 pathway. Recently, Zhang et al. (Zhang et al., 2019) found an F-box protein, RAE1,  
51 496 promoting the degradation of STOP1 via the 26S-proteasome pathway. The RAE1  
52 497 protein interacts with and triggers the 26S-proteasome-dependent degradation of

1  
2  
3 498 STOP1. Compared to the WT, seedlings homozygous for the loss-of-function *rae1*  
4 499 mutation accumulate more STOP1 proteins and *ALMT1* mRNAs. When grown under  
5 500 -Pi condition, the *rae1* seedlings have a primary root shorter than that of the WT, and  
6 501 when grown with toxic amount of Al it is longer. RAE1 is therefore a strong candidate  
7 502 mediating STOP1 degradation in our Fe- and Al-depleted growth conditions.  
8 503

9 504 The RAE1 and STOP1 proteins do not contain an obvious Fe- or Al-binding domain.  
10 505 How Al<sup>3+</sup> is sensed in plant is not known (Kochian et al., 2015) and thus the  
11 506 activation of STOP1 by Al<sup>3+</sup> remains an open question. But, since both Fe and Al<sup>3+</sup>  
12 507 stimulate the accumulation of STOP1 in the nucleus with similar kinetics, in the same  
13 508 root cells and only under acidic conditions, it is tempting to speculate that these two  
14 509 cations share a sensing mechanism. Further work will be needed to understand this  
15 510 mechanism.  
16 511

## 17 512 **Conclusion**

18 513 In acidic soils, toxic Al<sup>3+</sup> and Fe, in conjunction with Pi-deficiency limit crops growth  
19 514 (Kochian, 2004). There are increasing evidences that, at the cellular level, toxic Al<sup>3+</sup>  
20 515 share some common targets and processes with the effects of Fe cations in acidic  
21 516 and low-Pi conditions (Abel, 2017). We now demonstrate that Al<sup>3+</sup> and Fe also share  
22 517 at least one signalling step: STOP1 accumulation in the nucleus. Our study therefore  
23 518 contributes to further dissection of the sensing and signalling pathways of Al and Fe  
24 519 in plants.  
25 520  
26 521

## 27 522 **Experimental procedures**

### 28 523 **Plant material.**

29 524 The Arabidopsis wild-type (*Col<sup>er105</sup>*), *pALMT1::GUS<sub>#2</sub>*, *pSTOP1::GFP-STOP1<sub>#B10</sub>* and  
30 525 *als3*; *pSTOP1::GFP-STOP1<sub>#B10</sub>* lines were described previously (Balzergue et al.,  
31 526 2017, Wang et al., 2019); *pSPX1::GUS* is in the Col-0 background (Duan et al.,  
32 527 2008).  
33 528

### 34 529 **Seedling growth.**

35 530 Seeds were surface-sterilised 5 min in a solution containing 70% ethanol and 0.05%  
36 531 sodium dodecyl sulfate, and washed twice with ethanol 96%. The nutrient solution  
37 532 was as previously (Balzergue et al., 2017). The agar (8 g l<sup>-1</sup>) and agarose (7 g l<sup>-1</sup>) for  
38 533 plates was from Sigma-Aldrich (A1296 #BCBL6182V) and Lonza (Seakem LE  
39 534 agarose) respectively. The media were buffered at pH ranging from 5.5-6.8 with  
40 535 3.4 mM 2-(*N*-morpholino) ethane sulfonic acid. The different plates were prepared by  
41 536 mixing the melted autoclaved 1X agar or agarose medium (composition as above)  
42 537 with the buffer. Solutions of AlCl<sub>3</sub> and FeCl<sub>2</sub> were sterilized by filtration before adding  
43 538 to the plates.  
44 539

45 540 For GFP fluorescence experiments, five seeds were sown on a piece of sterile nylon  
46 541 square (1 cm X 1 cm, mesh size 10 μm) itself lying on the agar plate. After 3 days of  
47 542 growth on the agar plate, the nylon meshes carrying the seedlings were transferred  
48 543 on the new plates containing or not different concentrations of aluminium or iron.

49 544 For the experiments with MG132, nylon meshes carrying the 3 days old seedlings  
50 545 were transferred on 10 μl droplet (liquid extracted from Sigma-Aldrich agar (A1296  
51 546 #BCBL6182V) from which the seedlings were pre-grown) containing or not different  
52 547  
53 548  
54 549  
55 550  
56 551  
57 552  
58 553  
59 554  
60 555

1  
2  
3 547 concentration of MG132. In all experiments, the pH of the growth media for  
4 548 germination and for the subsequent transfer was identical.

5 549  
6 550 For the qRT–PCR experiment, seeds were sown side by side in a line, on a 5 cm  
7 551 strip of nylon meshes. Three to 3.5 days after sowing the whole roots of seedlings  
8 552 were harvested and mRNA extracted.

9 553

#### 10 554 **Agar treatment with deferoxamine B (DFO)**

11 555 To reduce bioavailable iron in the growth media, we used two methods. For the DFO-  
12 556 agar, 100  $\mu$ M of deferoxamine B (DFO) was added to the 1x melted autoclaved  
13 557 growth media, just before pouring the plates. For the washed DFO-treated agar, we  
14 558 prepared the agar as follow: 4 g of Sigma-Aldrich agar (A1296 #BCBL6182V) was  
15 559 added to 100 ml of milliQ water containing 600  $\mu$ M of DFO and stirred during 15 h.  
16 560 The agar was then washed by centrifugation (520 rcf) through a nylon mesh (mesh  
17 561 size 10  $\mu$ m); this washing step with milliQ water was carried out twice. This washed  
18 562 DFO-agar was then used to prepare the growth plates.

19 563

#### 20 564 **Quantification of Al, Fe and P in the agars and agarose**

21 565 Dried samples of agars and agarose were mineralized by addition of 300  $\mu$ L HNO<sub>3</sub>  
22 566 70% (ICP grade, JT Baker) by incubation overnight in an oven at 80 °C. The  
23 567 solutions were diluted to a final volume of 5 mL by addition of distilled water. The Al,  
24 568 Fe and P were quantified with Inductively Coupled Plasma – Absorption Emission  
25 569 Spectrometer (ICP-AES 5110 SVDV, Agilent Technologies). The concentrations of  
26 570 metals were determined using standard curves obtained from solutions made with  
27 571 ICP-grade elements.

28 572

#### 29 573 **Quantitative RT–PCR.**

30 574 Total RNA were extracted from whole roots using the Direct-Zol™ RNA MiniPrep  
31 575 (ZYMO research, USA) and treated with the RNase-free DNase Set (ZYMO  
32 576 research, USA) according to the manufacturer's instructions. Reverse transcription  
33 577 was performed on 500 ng of total RNA using the qScript™ cDNA SuperMix (Quanta  
34 578 Bioscience™). Quantitative PCR (qRT–PCR) was performed on a 480 LightCycler  
35 579 thermocycler (Roche) using the manufacturer's instructions with Light cycler 480sybr  
36 580 green I master (Roche) and with primers listed in Table S2. We used Tubulin gene  
37 581 (At5g62690) as a reference gene for normalization and the quantification of gene  
38 582 expression was as according the published method (Pfaffi, 2001).

39 583

#### 40 584 **GUS histochemical staining.**

41 585 The GUS staining of Arabidopsis seedlings was conducted as previously described  
42 586 (Balzergue et al., 2017), except that the seedlings were incubated 40 min in the GUS  
43 587 staining solution.

44 588

#### 45 589 **Quantification of GFP fluorescence.**

46 590 Images were collected on a Zeiss LSM780 confocal microscope (Carl Zeiss, France)  
47 591 using a  $\times$  20 dry objective (Plan Apo NA 0.80). GFP were excited with the argon ion  
48 592 laser (488 nm). Emitted light was collected from 493 to 538 nm for GFP, using the  
49 593 MBS 488 filter. All nuclei were imaged using the same conditions of gain, offset,  
50 594 resolution and with a pinhole setting of 1 a.u. The quantification of GFP fluorescence  
51 595 was carried out as follows: a Z-stack of 9 images (separated by 1.8  $\mu$ m distance)  
52 596 imaged representative nuclei on the surface of the root. Images were acquired in 12

bits using Zen black software (Zen black 2012 SP2 Version 11.0), then converted to a maximal projection image. The average nuclei fluorescence intensities were quantified using the Zen blue software (Zen 2 blue edition, version 2.0.0.0), by drawing identical ROI (region of interest). A 120  $\mu\text{m}$  X 60  $\mu\text{m}$  rectangle was defined at 200  $\mu\text{m}$  from a root tip (roughly in the transition zone), in which a region of interest (6  $\mu\text{m}$  X 6  $\mu\text{m}$ ) inside each nucleus was defined for the measurement of fluorescence.

## Acknowledgements

B.Alonso, S.Chiarenza, H.Javot and N.Léonhardt (CEA, cadarache) for experimental helps and discussions.

This work was funded by CEA, Investissements d'avenir (DEMETERRES) and ROULLIER/AGRO INNOVATION INTERNATIONAL (C.M.); X.W. and D.L. were funded by The National Natural Science Foundation of China (grant no. 31670256). Support for the microscopy equipment was provided by the Région Provence Alpes Côte d'Azur, the Conseil General of Bouches du Rhône, the French Ministry of Research, the CNRS and the Commissariat à l'Energie Atomique et aux Energies Alternatives. The qRT-PCR machine was funded by Hélobiotech.

The authors declare no competing interests.

## Short legends for Supporting Information

### Figure S1

Under neutral condition, *ALMT1* is not expressed.

Picture of the root tip after the GUS staining, of WT seedlings carrying the *pALMT1::GUS* marker. Seedlings were grown in low-Pi at pH 5.8 or 7.1, with or without 15  $\mu\text{M}$  Fe. Note that at pH 7.1 no GUS staining is detected. Bar, 1 mm.

### Figure S2

Expression (qRT-PCR) of *ALMT1*, *SPX1* and *PPsPase* in seedlings roots. Seedlings were grown 3 days on the indicated media. Mean  $\pm$ SD ( $n$  = two independent experiments).

### Figure S3

Analysis of *STOP1* mRNA expression.

WT seedlings were pre-grown 3 days under low-Pi condition at pH 5.8 or 7 without Fe or Al added, transferred for 3 hours in the same original pH condition with or without  $\text{Al}^{3+}$  or  $\text{Fe}^{2+}$  before extraction of root RNAs and qRT-PCR reactions. The conditions for qRT-PCR reactions and the calculations of relative expression were as in Figure 3 and Figure S2. Mean  $\pm$ SD ( $n$  = two independent experiments). *ALMT1* was used as a control.

### Figure S4

Fe promotes the accumulation of GFP-STOP1 in root nuclei.

The GFP fluorescence was measured (a.u.) in nuclei at the root tip of *pSTOP1::GFP-STOP1* seedlings.

a) Three-day-old seedlings were transferred 2 h in -Pi plates with the indicated concentration of Fe.



1  
2  
3 646 b) Three-day-old seedlings were transferred for the indicated time in -Pi plates  
4 647 containing 0 or 60  $\mu\text{M}$  Fe.

5 648 c) Three-day-old seedlings were transferred 2h in -Pi plates buffered at the indicated  
6 649 pH, containing 0 or 60  $\mu\text{M}$  Fe.

7 650 d) Picture of GFP fluorescence at the root tip, in seedlings transferred 2h in -Pi plates  
8 651 without (left) or with (right) 60  $\mu\text{M}$  Fe.

9 652  
10 653 Box plots indicate the median, the 25<sup>th</sup> to 75<sup>th</sup> percentiles (box edges) and the min to  
11 654 max range (whiskers); Mann-Whitney test; \*\*\*\* $P < 0.0001$ ; NS, not significant  
12 655 ( $P > 0.05$ ); number of nuclei per condition: a) 329-346; b) 291-343; c) 322-392).

### 656 657 **Figure S5**

658 Non-transgenic WT seedlings were grown on a -Pi-Fe plate made with the DFO-agar,  
659 transferred to a -Pi plate containing 0 or 60  $\mu\text{M}$  Fe for 2 h, and the fluorescence  
660 pictured by confocal microscopy (same setting as in Figure S9). Note the small  
661 autofluorescent dots. Bar, 100  $\mu\text{m}$ .

### 662 663 **Figure S6**

664 The 26S proteasome inhibitor MG132 promotes GFP-STOP1 accumulation in root  
665 nuclei.

666 Three days old seedlings were treated 6 h (a) or 4 h (b), without or with 60, 125 or  
667 250  $\mu\text{M}$  (a) or 250  $\mu\text{M}$  (b) MG132, and photographed as in Figure 4b. **a** and **b**  
668 represent two independent experiments. Bars, 100  $\mu\text{m}$ .

### 669 670 **Figure S7**

671 Aluminum stimulates the expression of *pALMT1::GUS*.

672  
673 Seedlings were grown four days on a -Pi medium pH 5.5, made with a washed DFO-  
674 treated agar, supplemented or not with 15  $\mu\text{M}$   $\text{Al}^{3+}$ , before GUS staining. Note that  
675 the 0 Al control is the same as in Figure 2b, since it is part of the same experiment.  
676 Bar, 1 mm.

### 677 678 **Figure S8**

679  $\text{Al}^{3+}$  promotes the accumulation of GFP-STOP1 in root nuclei.

680  
681 The GFP fluorescence was measured (a.u.) in nuclei at the root tip of pSTOP1::GFP-  
682 STOP1 seedlings.

683 a) Three-day-old seedlings were transferred 2 h in -Pi plates with the indicated  
684 concentration of  $\text{Al}^{3+}$ .

685 b) Three-day-old seedlings were transferred for the indicated time in -Pi plates  
686 containing 0 or 30  $\mu\text{M}$   $\text{Al}^{3+}$ .

687 c) Three-day-old seedlings were transferred 2h in -Pi plates buffered at the indicated  
688 pH, containing 0 or 30  $\mu\text{M}$   $\text{Al}^{3+}$ .

689  
690 Box plots indicate the median, the 25<sup>th</sup> to 75<sup>th</sup> percentiles (box edges) and the min to  
691 max range (whiskers); Mann-Whitney test; \*\*\*\* $P < 0.0001$ ; number of nuclei per  
692 condition: a) 315-348; b) 330-399; c) 315-448).

### 693 694 **Figure S9**

695 ALS3 represses STOP1 accumulation in root nuclei.

1  
2  
3 696 a) WT and the *als3* mutant seedlings carrying the *pSTOP1::GFP-STOP1* construct  
4 697 were grown 3 days on a -Pi-Fe plate, transferred to -Pi or -Pi-Fe plates for 2 h, and  
5 698 GFP-fluorescence was pictured by confocal microscopy. Bars, 100  $\mu$ m.  
6 699

## 700 References

- 701 Abel S, 2017. Phosphate scouting by root tips. *Curr Opin Plant Biol* **39**, 168-77.  
702 Balzergue C, Darteville T, Godon C, *et al.*, 2017. Low phosphate activates STOP1-ALMT1  
703 to rapidly inhibit root cell elongation. *Nat Commun* **8**, 15300.  
704 Bouain N, Shahzad Z, Rouached A, *et al.*, 2014. Phosphate and zinc transport and  
705 signalling in plants: toward a better understanding of their homeostasis interaction. *J*  
706 *Exp Bot.* **65**, 5725-41.  
707 Briat JF, Rouached H, Tissot N, Gaymard F, Dubos C, 2015. Integration of P, S, Fe, and Zn  
708 nutrition signals in *Arabidopsis thaliana*: potential involvement of PHOSPHATE  
709 STARVATION RESPONSE 1 (PHR1). *Front Plant Sci* **6**, 290.  
710 Che J, Tsutsui T, Yokosho K, Yamaji N, Ma JF, 2018. Functional characterization of an  
711 aluminum (Al)-inducible transcription factor, ART2, revealed a different pathway for Al  
712 tolerance in rice. *New Phytol* **220**, 209-18.  
713 Daspute AA, Kobayashi Y, Panda SK, *et al.*, 2018. Characterization of CcSTOP1; a C2H2-  
714 type transcription factor regulates Al tolerance gene in pigeonpea. *Planta* **247**, 201-14.  
715 Dong J, Pineros MA, Li X, *et al.*, 2017. An *Arabidopsis* ABC Transporter Mediates  
716 Phosphate Deficiency-Induced Remodeling of Root Architecture by Modulating Iron  
717 Homeostasis in Roots. *Mol Plant* **10**, 244-59.  
718 Duan K, Yi K, Dang L, Huang H, Wu W, Wu P, 2008. Characterization of a sub-family of  
719 *Arabidopsis* genes with the SPX domain reveals their diverse functions in plant  
720 tolerance to phosphorus starvation. *Plant J* **54** 965-75.  
721 Fan W, Lou HQ, Gong YL, *et al.*, 2015. Characterization of an inducible C2H2-type zinc  
722 finger transcription factor VuSTOP1 in rice bean (*Vigna umbellata*) reveals differential  
723 regulation between low pH and aluminum tolerance mechanisms. *New Phytologist* **208**,  
724 456-68.  
725 Gutiérrez-Alanís D, Yong-Villalobos L, Jiménez-Sandoval P, *et al.*, 2017. Phosphate  
726 Starvation-Dependent Iron Mobilization Induces CLE14 Expression to Trigger Root  
727 Meristem Differentiation through CLV2/PEPR2 Signaling. *Dev Cell* **41**, 555-70.  
728 Hanchi M, Thibaud MC, Legeret B, *et al.*, 2018. The Phosphate Fast-Responsive Genes  
729 PECP1 and PPsPase1 Affect Phosphocholine and Phosphoethanolamine Content. *Plant*  
730 *Physiol* **176**, 2943-62.  
731 Hindt MN, Akmakjian GZ, Pivarski KL, *et al.*, 2017. BRUTUS and its paralogs, BTS LIKE1  
732 and BTS LIKE2, encode important negative regulators of the iron deficiency response in  
733 *Arabidopsis thaliana*. *Metallomics* **9**, 876-90.  
734 Hinsinger P, 2001. Bioavailability of soil inorganic P in the rhizosphere as affected by  
735 root-induced chemical changes: a review. *Plant soil* **237**, 173-95.  
736 Hirsch J, Marin E, Floriani M, *et al.*, 2006. Phosphate deficiency promotes modification of  
737 iron distribution in *Arabidopsis* plants. *Biochimie* **88**, 1767-71.  
738 Hoekenga OA, Maron LG, Pineros MA, *et al.*, 2006. AtALMT1, which encodes a malate  
739 transporter, is identified as one of several genes critical for aluminum tolerance in  
740 *Arabidopsis*. *Proc Natl Acad Sci U S A* **103**, 9738-43.  
741 Huang CF, Yamaji N, Ma JF, 2010. Knockout of a bacterial-type ATP-binding cassette  
742 transporter gene, AtSTAR1, results in increased aluminum sensitivity in *Arabidopsis*.  
743 *Plant Physiol* **153**, 1669-77.

- 1  
2  
3 744 Huang S, Gao J, You J, *et al.*, 2018. Identification of STOP1-Like Proteins Associated With  
4 745 Aluminum Tolerance in Sweet Sorghum (*Sorghum bicolor* L.). *Front Plant Sci* **9**, 258.  
5 746 Iuchi S, Koyama H, Iuchi A, *et al.*, 2007. Zinc finger protein STOP1 is critical for proton  
6 747 tolerance in Arabidopsis and coregulates a key gene in aluminum tolerance. *Proc Natl*  
7 748 *Acad Sci U S A* **104**, 9900-5.  
8 749 Kobayashi T, Itai RN, Aung MS, Senoura T, Nakanishi H, Nishizawa NK, 2012. The rice  
9 750 transcription factor IDEF1 directly binds to iron and other divalent metals for sensing  
10 751 cellular iron status. *Plant J* **69**, 81-91.  
11 752 Kobayashi T, Nagasaka S, Senoura T, Itai RN, Nakanishi H, Nishizawa NK, 2013a. Iron-  
12 753 binding haemerythrin RING ubiquitin ligases regulate plant iron responses and  
13 754 accumulation. *Nat Commun* **4**, 2792.  
14 755 Kobayashi T, Nishizawa NK, 2012. Iron uptake, translocation, and regulation in higher  
15 756 plants. *Annu Rev Plant Biol* **63**, 131-52.  
16 757 Kobayashi Y, Kobayashi Y, Watanabe T, *et al.*, 2013b. Molecular and physiological  
17 758 analysis of Al<sup>3+</sup> and H<sup>+</sup> rhizotoxicities at moderately acidic conditions. *Plant Physiol* **163**,  
18 759 180-92.  
19 760 Kochian LV, Hoekenga, O. A., Pineros, M. A., 2004. How do crop plants tolerate acid soils?  
20 761 Mechanisms of aluminum tolerance and phosphorous efficiency. *Annu Rev Plant Biol.* **55**,  
21 762 459-93.  
22 763 Kochian LV, Pineros MA, Liu JP, Magalhaes JV, 2015. Plant Adaptation to Acid Soils: The  
23 764 Molecular Basis for Crop Aluminum Resistance. *Annu Rev Plant Biol.* **66**, 571-98.  
24 765 Larsen PB, Geisler MJ, Jones CA, Williams KM, Cancel JD, 2005. ALS3 encodes a phloem-  
25 766 localized ABC transporter-like protein that is required for aluminum tolerance in  
26 767 Arabidopsis. *Plant J.* **41**, 353-63.  
27 768 Long TA, Tsukagoshi H, Busch W, Lahner B, Salt DE, Benfey PN, 2010. The bHLH  
28 769 transcription factor POPEYE regulates response to iron deficiency in Arabidopsis roots.  
29 770 *Plant Cell* **22**, 2219-36.  
30 771 Lynch JPB, K.M., 2001. Topsoil foraging - an architectural adaptation of plants to low  
31 772 phosphorus availability. *Plant and Soil* **237**, 225-37.  
32 773 Misson J, Raghothama KG, Jain A, *et al.*, 2005. A genome-wide transcriptional analysis  
33 774 using Arabidopsis thaliana Affymetrix gene chips determined plant responses to  
34 775 phosphate deprivation. *Proc Natl Acad Sci U S A* **102**, 11934-9.  
35 776 Mora-Macias J, Ojeda-Rivera JO, Gutierrez-Alanis D, *et al.*, 2017. Malate-dependent Fe  
36 777 accumulation is a critical checkpoint in the root developmental response to low  
37 778 phosphate. *Proc. Nat. Aca. Sci. USA* **114**, E3563-E72.  
38 779 Muller J, Toev T, Heisters M, *et al.*, 2015. Iron-dependent callose deposition adjusts root  
39 780 meristem maintenance to phosphate availability. *Dev Cell* **33**, 216-30.  
40 781 Pfaffi MW, 2001. A new mathematical model for relative quantification in real-time RT-  
41 782 PCR. *Nucleic Acids Res.* **29**, e45.  
42 783 Puga MI, Mateos I, Charukesi R, *et al.*, 2014. SPX1 is a phosphate-dependent inhibitor of  
43 784 PHOSPHATE STARVATION RESPONSE 1 in Arabidopsis. *Proc Natl Acad Sci U S A* **111**,  
44 785 14947-52.  
45 786 Puga MI, Rojas-Triana M, De Lorenzo L, Leyva A, Rubio V, Paz-Ares J, 2017. Novel signals  
46 787 in the regulation of Pi starvation responses in plants: facts and promises. *Curr Opin Plant*  
47 788 *Biol* **39**, 40-9.  
48 789 Reymond M, Svistoonoff S, Loudet O, Nussaume L, Desnos T, 2006. Identification of QTL  
49 790 controlling root growth response to phosphate starvation in Arabidopsis thaliana. *Plant*  
50 791 *Cell Environ* **29**, 115-25.  
51  
52  
53  
54  
55  
56  
57  
58  
59  
60



- 1  
2  
3 792 Sawaki Y, Iuchi S, Kobayashi Y, *et al.*, 2009. STOP1 regulates multiple genes that protect  
4 793 arabidopsis from proton and aluminum toxicities. *Plant Physiol* **150**, 281-94.  
5 794 Sawaki Y, Kobayashi Y, Kihara-Doi T, *et al.*, 2014. Identification of a STOP1-like protein  
6 795 in Eucalyptus that regulate transcription of Al tolerance genes. *Plant Sci.* **223**, 8-15.  
7 796 Selote D, Samira R, Matthiadis A, Gillikin JW, Long TA, 2015. Iron-binding E3 ligase  
8 797 mediates iron response in plants by targeting basic helix-loop-helix transcription  
9 798 factors. *Plant Physiol* **167**, 273-86.  
10 799 Singh AP, Fridman Y, Friedlander-Shani L, Tarkowska D, Strnad M, Savaldi-Goldstein S,  
11 800 2014. Activity of the brassinosteroid transcription factors BRASSINAZOLE RESISTANT1  
12 801 and BRASSINOSTEROID INSENSITIVE1-ETHYL METHANESULFONATE-  
13 802 SUPPRESSOR1/BRASSINAZOLE RESISTANT2 blocks developmental reprogramming in  
14 803 response to low phosphate availability. *Plant Physiol* **166**, 678-88.  
15 804 Singh AP, Fridman Y, Holland N, *et al.*, 2018. Interdependent Nutrient Availability and  
16 805 Steroid Hormone Signals Facilitate Root Growth Plasticity. *Dev Cell* **46**, 59-72 e4.  
17 806 Svistoonoff S, Creff A, Reymond M, *et al.*, 2007. Root tip contact with low-phosphate  
18 807 media reprograms plant root architecture. *Nat Genet* **39**, 792-6.  
19 808 Thibaud MC, Arrighi JF, Bayle V, *et al.*, 2010. Dissection of local and systemic  
20 809 transcriptional responses to phosphate starvation in Arabidopsis. *Plant J* **64**, 775-89.  
21 810 Ticconi CA, Delatorre CA, Lahner B, Salt DE, Abel S, 2004. Arabidopsis pdr2 reveals a  
22 811 phosphate-sensitive checkpoint in root development. *Plant J* **37**, 801-14.  
23 812 Ticconi CA, Lucero RD, Sakhonwasee S, *et al.*, 2009. ER-resident proteins PDR2 and LPR1  
24 813 mediate the developmental response of root meristems to phosphate availability. *Proc*  
25 814 *Natl Acad Sci U S A* **106**, 14174-9.  
26 815 Vert G, Grotz N, Dedaldechamp F, *et al.*, 2002. IRT1, an Arabidopsis transporter essential  
27 816 for iron uptake from the soil and for plant growth. *Plant Cell* **14**, 1223-33.  
28 817 Wang JJ, Hou QQ, Li PH, *et al.*, 2017. Diverse functions of multidrug and toxin extrusion  
29 818 (MATE) transporters in citric acid efflux and metal homeostasis in *Medicago truncatula*.  
30 819 *Plant Journal* **90**, 79-95.  
31 820 Wang X, Wang Z, Zheng Z, *et al.*, 2019. Genetic Dissection of Fe-Dependent Signaling in  
32 821 Root Developmental Responses to Phosphate Deficiency. *Plant Physiol* **179**, 300-16.  
33 822 Ward JT, Lahner B, Yakubova E, Salt DE, Raghothama KG, 2008. The effect of iron on the  
34 823 primary root elongation of Arabidopsis during phosphate deficiency. *Plant Physiol* **147**,  
35 824 1181-91.  
36 825 Wu W, Lin Y, Chen Q, *et al.*, 2018. Functional Conservation and Divergence of Soybean  
37 826 GmSTOP1 Members in Proton and Aluminum Tolerance. *Front Plant Sci* **9**, 570.  
38 827 Yamaji N, Huang CF, Nagao S, *et al.*, 2009. A zinc finger transcription factor ART1  
39 828 regulates multiple genes implicated in aluminum tolerance in rice. *Plant Cell* **21**, 3339-  
40 829 49.  
41 830 Zhang Y, Zhang J, Guo J, *et al.*, 2019. F-box protein RAE1 regulates the stability of the  
42 831 aluminum-resistance transcription factor STOP1 in Arabidopsis. *Proc Natl Acad Sci U S A*  
43 832 **116**, 319-27.  
44 833  
45 834  
46 835  
47 836  
48 837  
49 838  
50 839  
51 840

**Table S1:** Al, Fe and P content ( $\mu\text{g}/100\text{ mg}$  agar or agarose)

	Al	Fe	P
Agar Sigma A1296	5,75	3,82	5,86
Agar Sigma A1296 treated with DFO and washed	5,87	3,50	0,63
Agarose Ionza Seakem	0,42	0,24	0,81

**Table S2:** primers sequence

gene	primer	sequence (5' to 3')
<i>PPsPase1</i>	AT1G73010_R	GACGACACGTGGATGAATTG
	AT1G73010_F	TCATGATCAAGGCAAAACCA
<i>SPX1</i>	AT5G20150_R	GCGGCAATGAAAACACACTA
	AT5G20150_F	CGGGTTTTGAAGGAGATCAG
<i>IRT1</i>	AT4G19690_R	GACGATAGAACTATACTGCCTTGA
	AT4G19690_F	TGCGGAATTGAAATCATGTG
<i>ALMT1</i>	AT1G08430_R	CGATTCCGAGCTCATTCTTC
	AT1G08430_F	GGCAGTGTGCCTACAGGATT
<i>STOP1</i>	AT1G34370_F	AAGTGGCTTTGTTCTGTGG
	AT1G34370_R	GGCTGTGTGGTTTCTTGTT
<i>Tubulin</i>	AT5G62690_R	ACACCAGACATAGTAGCAGAAATCAAG
	AT5G62690_F	GAGCCTTACAACGCTACTCTGTCTGTC

## Figure legends

### Figure 1

Antagonistic interactions of Pi and Fe on the expression of *pALMT1::GUS*.

a) Effect of the Pi concentration on GUS staining, when Fe is at 15  $\mu$ M.

b) Effect of the Fe concentration on GUS staining, when Pi is at 250  $\mu$ M.

Seedling were grown 3 days on a pH 6.7 medium not supplemented with Pi and Fe, and transferred 24 h on a pH 5.5 medium supplemented with the indicated concentrations of Pi and Fe, before GUS staining. Bar, 1 mm.

### Figure 2

Fe is necessary for the expression of *ALMT1*.

a) DFO inhibits the expression of *pALMT1::GUS*.

b) In a growth medium made with a washed DFO-treated agar, supplementation of Fe restores the expression of *pALMT1::GUS*.

Seedling were grown 4 days on a pH 5.5 medium not supplemented with Pi, and supplemented or not with the indicated concentrations of DFO and Fe, before GUS staining. Bar, 1 mm.

### Figure 3

Fe, but not the -Pi condition *per se*, stimulates the expression of *pALMT1::GUS*.

a) GUS staining in the primary root of *pALMT1::GUS* and *pSPX1::GUS* seedlings.

b) Expression (qRT-PCR) of *ALMT1*, *SPX1*, *IRT1* and *PPsPase* in seedlings roots (mean of three technical replicates).

1  
2  
3 871 Seedlings were grown 5 days (for the GUS staining experiment) or 3.5 days (for the  
4 872 qRT-PCR experiment) on a medium not supplemented with Pi and Fe, at pH 6.7 or  
5 873 5.5. Bars, 1 mm.

#### 8 875 **Figure 4**

9 876 Fe promotes the accumulation of GFP-STOP1 in root nuclei

10 877  
11 878 The GFP fluorescence was measured (a.u.) in nuclei at the root tip of *pSTOP1::GFP-*  
12 879 *STOP1* seedlings.

13 880 a) Top: three-day-old seedlings were transferred 2 h in -Pi plates with the indicated  
14 881 concentration of Fe. Bottom: representative pictures used for measurements.

15 882  
16 883 b) MG132 promotes the accumulation of GFP-STOP1 in nuclei of the root tip.  
17 884 Seedlings carrying the *pSTOP1::GFP-STOP1* reporter were grown 3 days in agar  
18 885 (Agar Sigma A1296, Table S1). under low-Pi without Fe or Al added. Then, they were  
19 886 treated 4 h with or without 250  $\mu\text{M}$  MG132 before photographed with the confocal  
20 887 microscope. One representative picture is shown for each condition (see Figure S6  
21 888 for additional pictures). Note that under in the untreated control, STOP1 slightly  
22 889 accumulates in the nucleus.

23 890 c) Left: three-day-old seedlings were transferred for the indicated time in -Pi plates  
24 891 containing 0 or 60  $\mu\text{M}$  Fe. Right: representative pictures used for measurements.

25 892 d) Top: three-day-old seedlings were transferred 2 h in -Pi plates buffered at the  
26 893 indicated pH, containing 0 or 60  $\mu\text{M}$  Fe. Bottom: representative pictures used for  
27 894 measurements.

28 895  
29 896 Box plots indicate the median, the 25<sup>th</sup> to 75<sup>th</sup> percentiles (box edges) and the min to  
30 897 max range (whiskers); Mann-Whitney test; \*\*\*\* $P < 0.0001$ ; \*\*\* $P < 0.001$ ; \* $P < 0.05$ ; NS,  
31 898 not significant ( $P > 0.05$ ); number of nuclei per condition: a) 94-154; b) 99-119; c) 87-  
32 899 121). Bars, 100  $\mu\text{m}$ .

#### 33 901 **Figure 5**

34 902  $\text{Al}^{3+}$  promotes the accumulation of GFP-STOP1 in root nuclei.

35 903  
36 904 The GFP fluorescence was measured (a.u.) in nuclei at the root tip of *pSTOP1::GFP-*  
37 905 *STOP1* seedlings.

38 906 a) Top: three-day-old seedlings were transferred 2 h in -Pi plates with the indicated  
39 907 concentration of  $\text{Al}^{3+}$ . Bottom: representative pictures used for measurements.

40 908 b) Left: three-day-old seedlings were transferred for the indicated time in -Pi plates  
41 909 containing 0 or 30  $\mu\text{M}$   $\text{Al}^{3+}$ . Right: representative pictures used for measurements.

42 910 c) Top: three-day-old seedlings were transferred 2 h in -Pi plates buffered at the  
43 911 indicated pH, containing 0 or 30  $\mu\text{M}$   $\text{Al}^{3+}$ . Bottom: representative pictures used for  
44 912 measurements.

45 913 Box plots indicate the median, the 25<sup>th</sup> to 75<sup>th</sup> percentiles (box edges) and the min to  
46 914 max range (whiskers); Mann-Whitney test; \*\*\*\* $P < 0.0001$ ; \*\* $P < 0.01$ ; NS, not  
47 915 significant ( $P > 0.05$ ); number of nuclei per condition: a) 80-143; b) 102-125; c) 86-  
48 916 121). Bars, 100  $\mu\text{m}$ .

#### 49 917 **Figure 6**

50 918 ALS3 represses STOP1 accumulation in root nuclei.

51 919  
52 920

1  
2  
3 921 WT and the *als3* mutant seedlings carrying the *pSTOP1::GFP-STOP1* construct were  
4 922 grown 3 days on a -Pi-Fe plate (made with agar Seakem), transferred to -Pi-Fe or -  
5 923 Pi + 60 $\mu$ M Fe plates for 2 h, and GFP-fluorescence was visualized by confocal  
6 924 microscopy. To avoid saturated GFP fluorescence in the images, the microscope  
7 925 was set on the highest fluorescence (as detected in *als3*). Bars = 100  $\mu$ m.  
8 926

### 9 927 **Figure 7**

10 928 Model depicting the roles of Fe and Al on the STOP1 signalling and root growth in  
11 929 relation with Pi availability.  
12 930

13 931 Phosphate reversibly inactivates Fe and Al by forming a complex with them. Under -  
14 932 Pi condition and low-pH, Fe, Al or another unknown molecule accumulates in the cell  
15 933 where it decreases proteasomal degradation of STOP1 thereby stimulating the  
16 934 accumulation of STOP1 in the nucleus; nuclear STOP1 activates the transcription of  
17 935 *ALMT1*. The tonoplast-anchored ALS3 and STAR1 proteins pump the Fe, Al or the  
18 936 unknown molecule from the cytosol to the vacuole compartment, thereby decreasing  
19 937 its concentration in the cytosol. This reduces the accumulation of STOP1 in the  
20 938 nucleus and therefore the transcription of *ALMT1*. The *ALMT1* transporter exudes  
21 939 malate in the apoplast where, together with Fe and the ferroxidase LPR1, they  
22 940 generate ROS that inhibit cell wall expansion. Exuded malate also chelates Al<sup>3+</sup>,  
23 941 therefore preventing its toxicity (not shown in the scheme).  
24 942

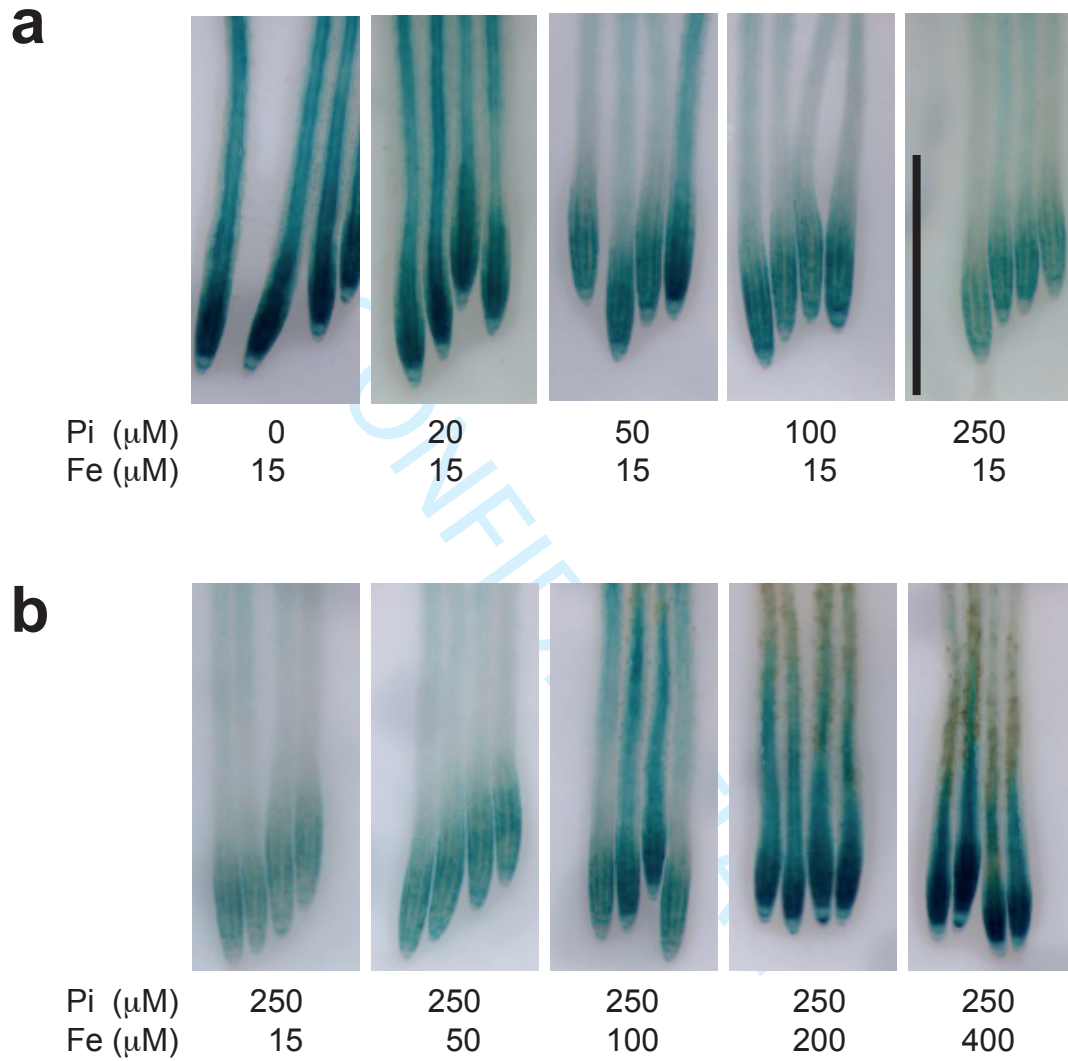
25 943 Red arrows: activation

26 944 Black arrow: proteasomal degradation

27 945 Blue blunt arrows: repression

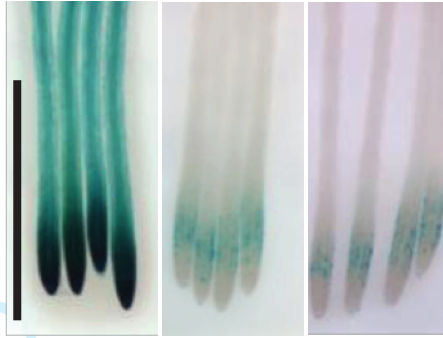
28 946 Dashed arrows: transfer between compartments  
29  
30  
31  
32  
33  
34  
35  
36  
37  
38  
39  
40  
41  
42  
43  
44  
45  
46  
47  
48  
49  
50  
51  
52  
53  
54  
55  
56  
57  
58  
59  
60

## Figure 1



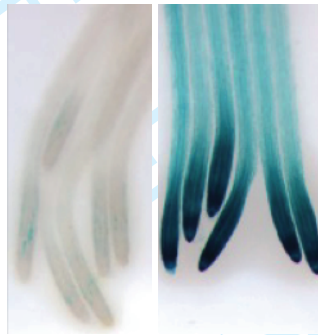
1  
2  
3  
4  
5  
6  
7  
8  
9  
10  
11  
12  
13  
14  
15  
16  
17  
18  
19  
20  
21  
22  
23  
24  
25  
26  
27  
28  
29  
30  
31  
32  
33  
34  
35  
36  
37  
38  
39  
40  
41  
42  
43  
44  
45  
46  
47  
48  
49  
50  
51  
52  
53  
54  
55  
56  
57  
58  
59  
60

**a**



DFO : 0                    100 $\mu$ M                    100 $\mu$ M  
Fe : 0                        0                                15 $\mu$ M

**b**

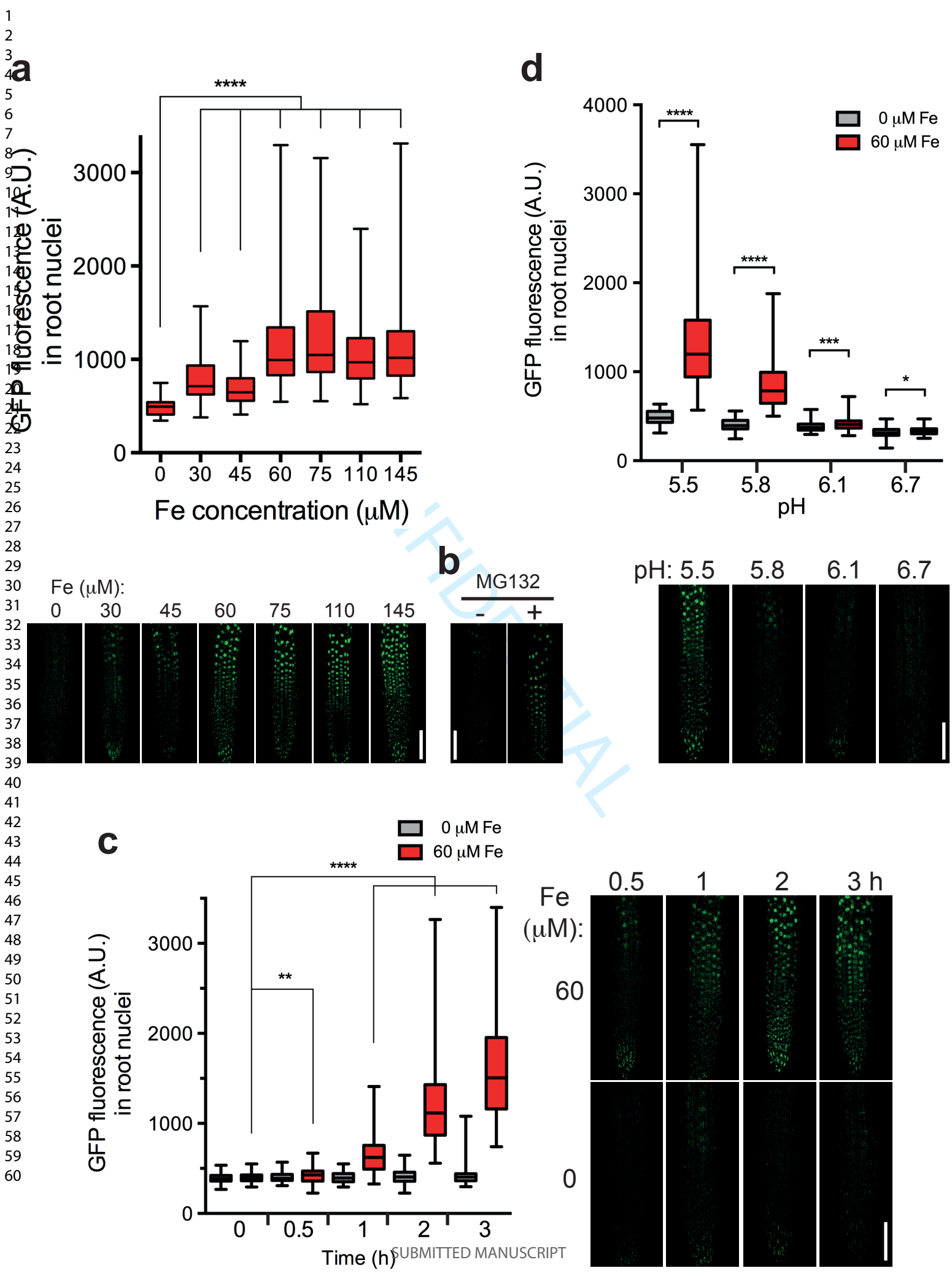


Fe : 0                        15 $\mu$ M

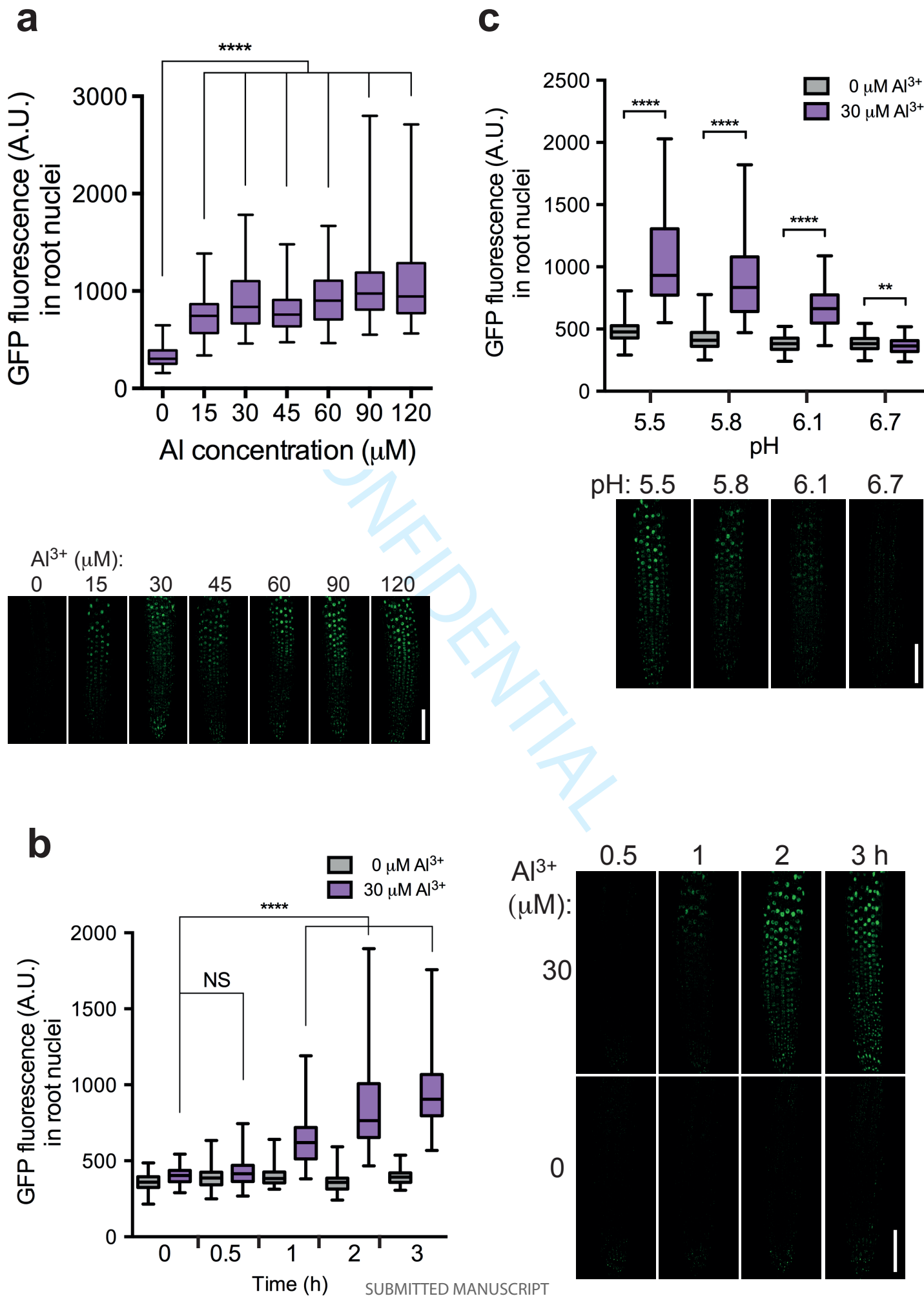




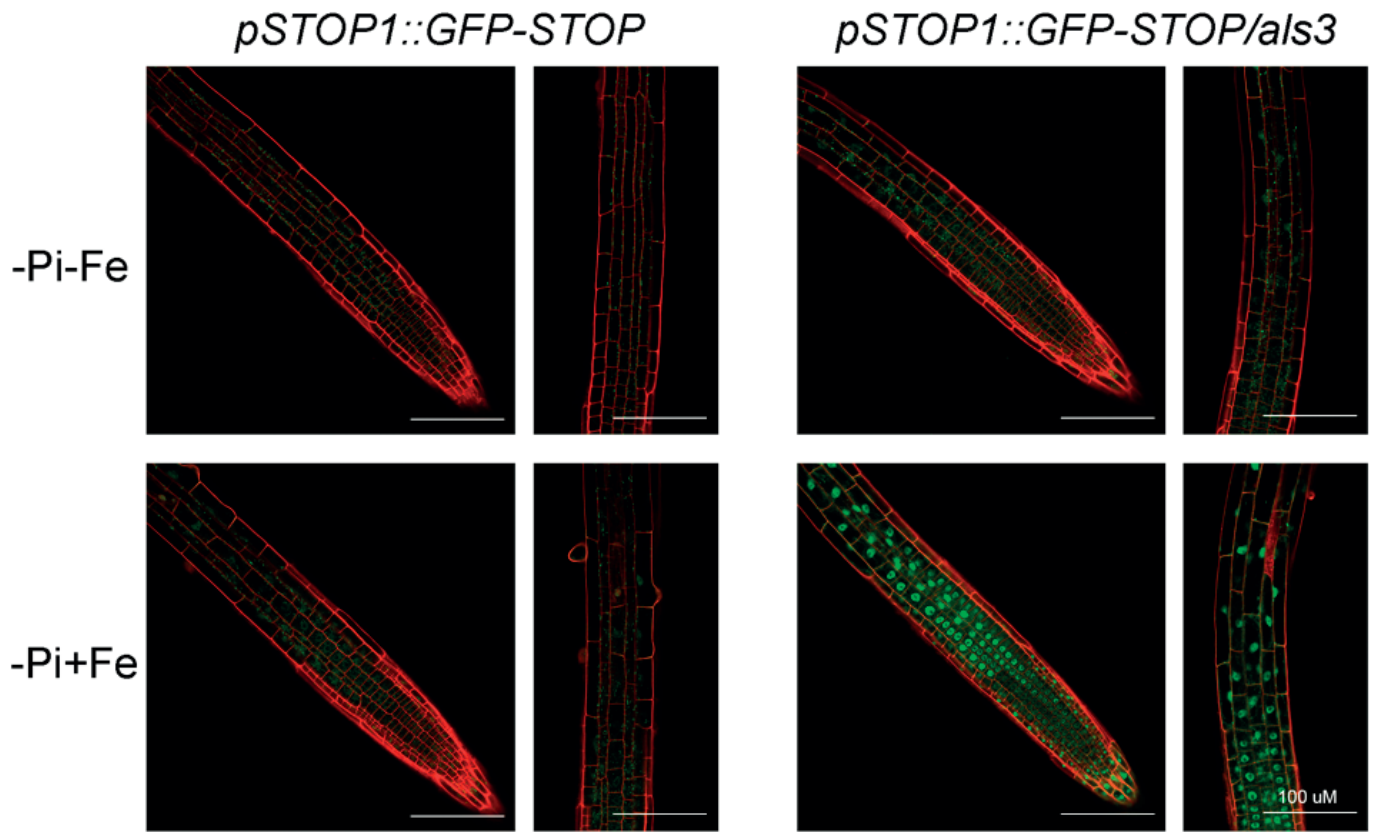




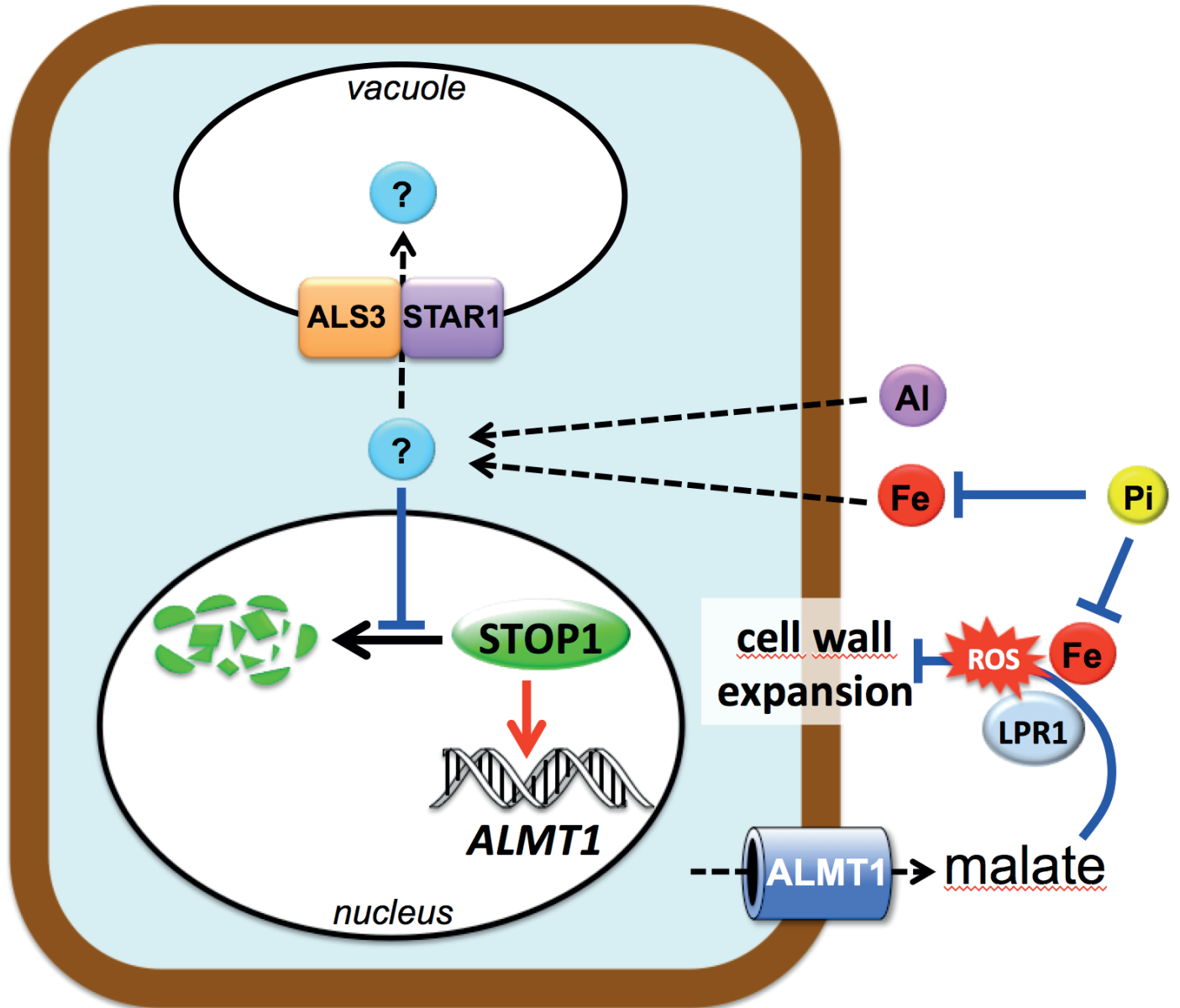
# Figure 5



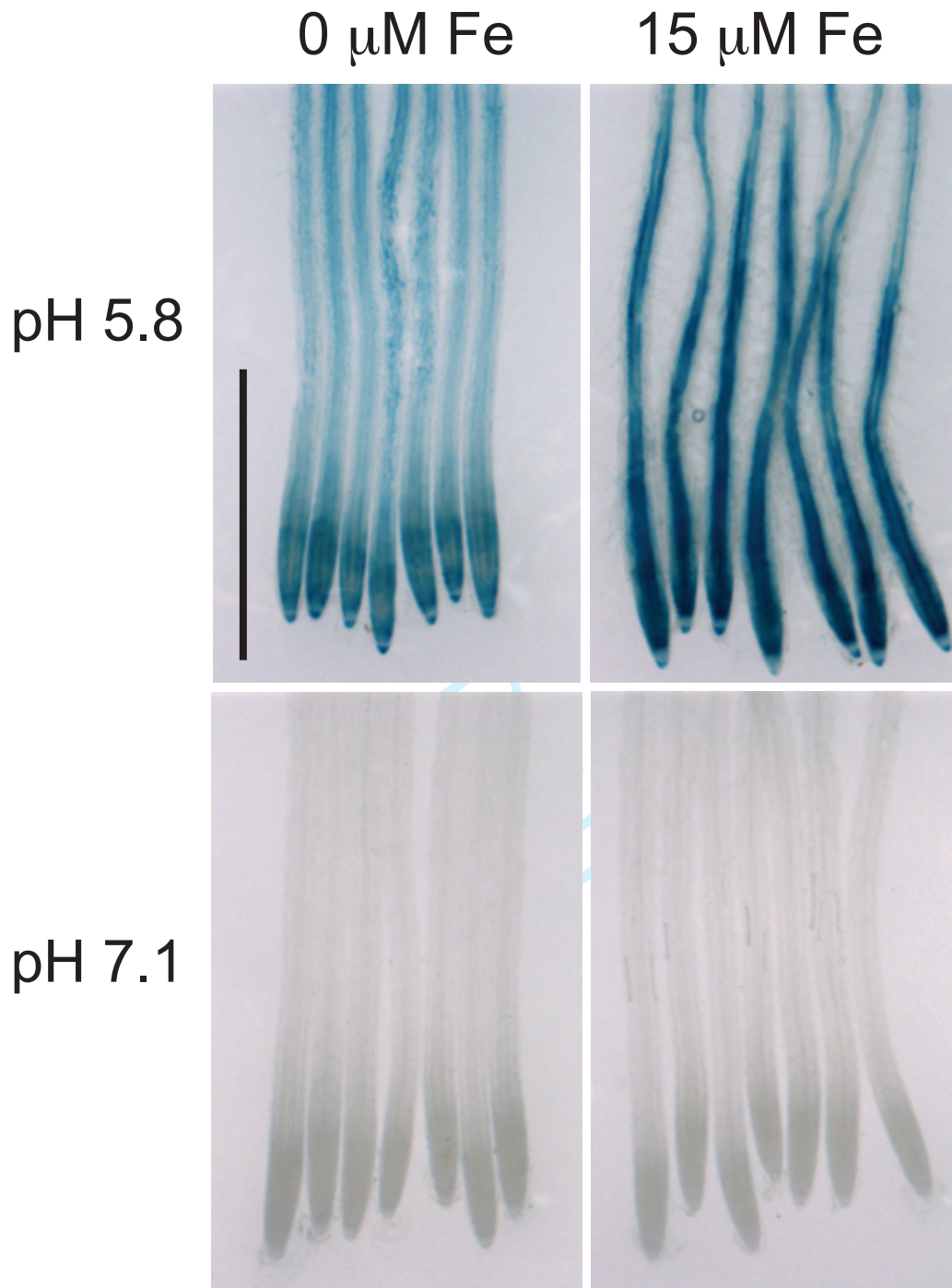
## Figure 6



## Figure 7



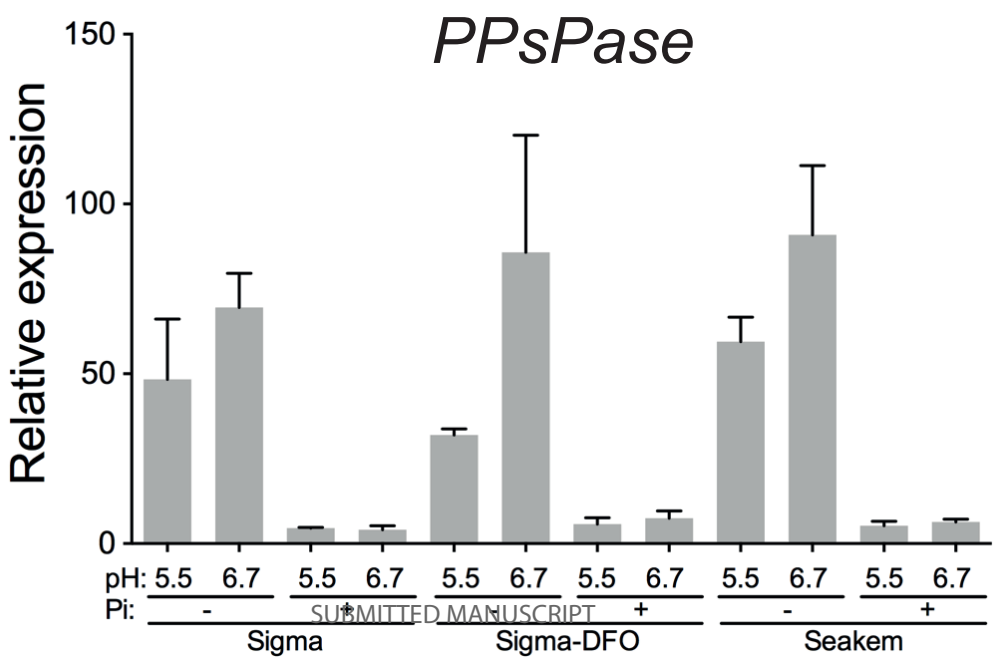
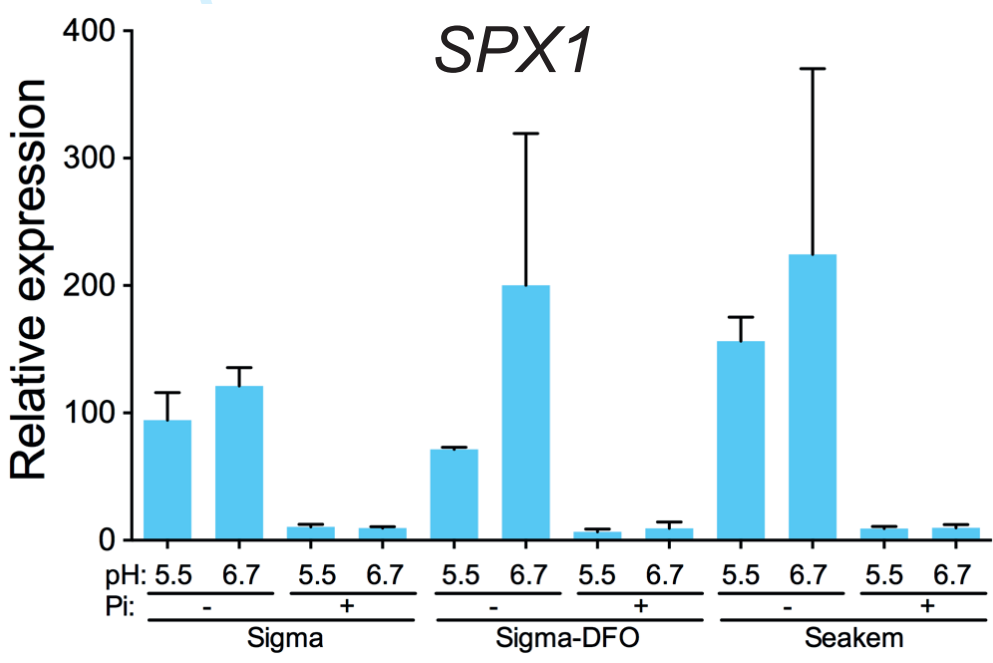
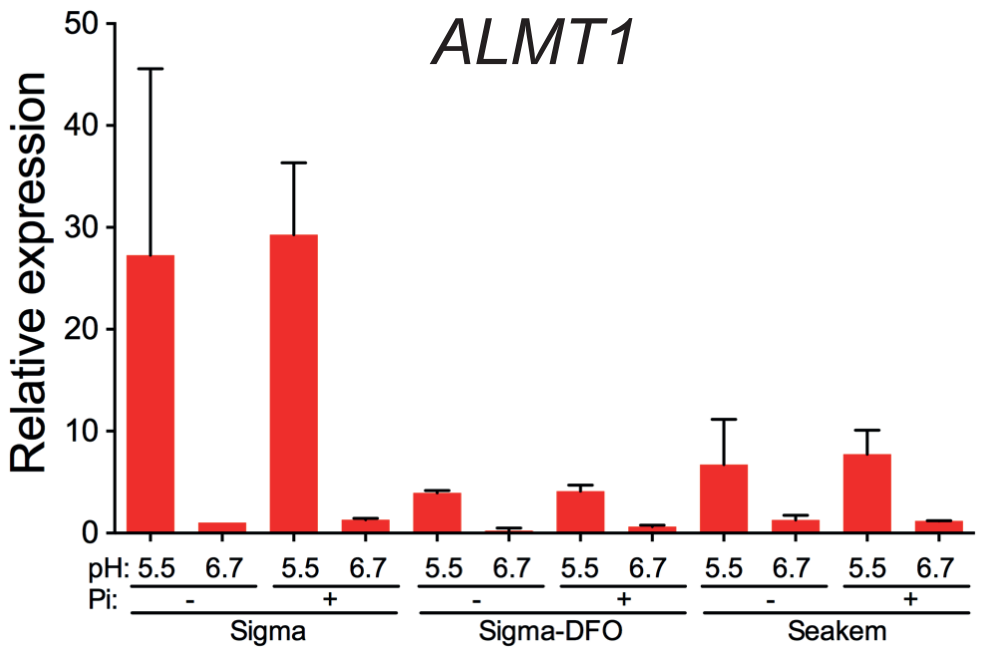
1  
2  
3  
4  
5  
6  
7  
8  
9  
10  
11  
12  
13  
14  
15  
16  
17  
18  
19  
20  
21  
22  
23  
24  
25  
26  
27  
28  
29  
30  
31  
32  
33  
34  
35  
36  
37  
38  
39  
40  
41  
42  
43  
44  
45  
46  
47  
48  
49  
50  
51  
52  
53  
54  
55  
56  
57  
58  
59  
60





# Figure S2

1  
2  
3  
4  
5  
6  
7  
8  
9  
10  
11  
12  
13  
14  
15  
16  
17  
18  
19  
20  
21  
22  
23  
24  
25  
26  
27  
28  
29  
30  
31  
32  
33  
34  
35  
36  
37  
38  
39  
40  
41  
42  
43  
44  
45  
46  
47  
48  
49  
50  
51  
52  
53  
54  
55  
56  
57  
58  
59  
60



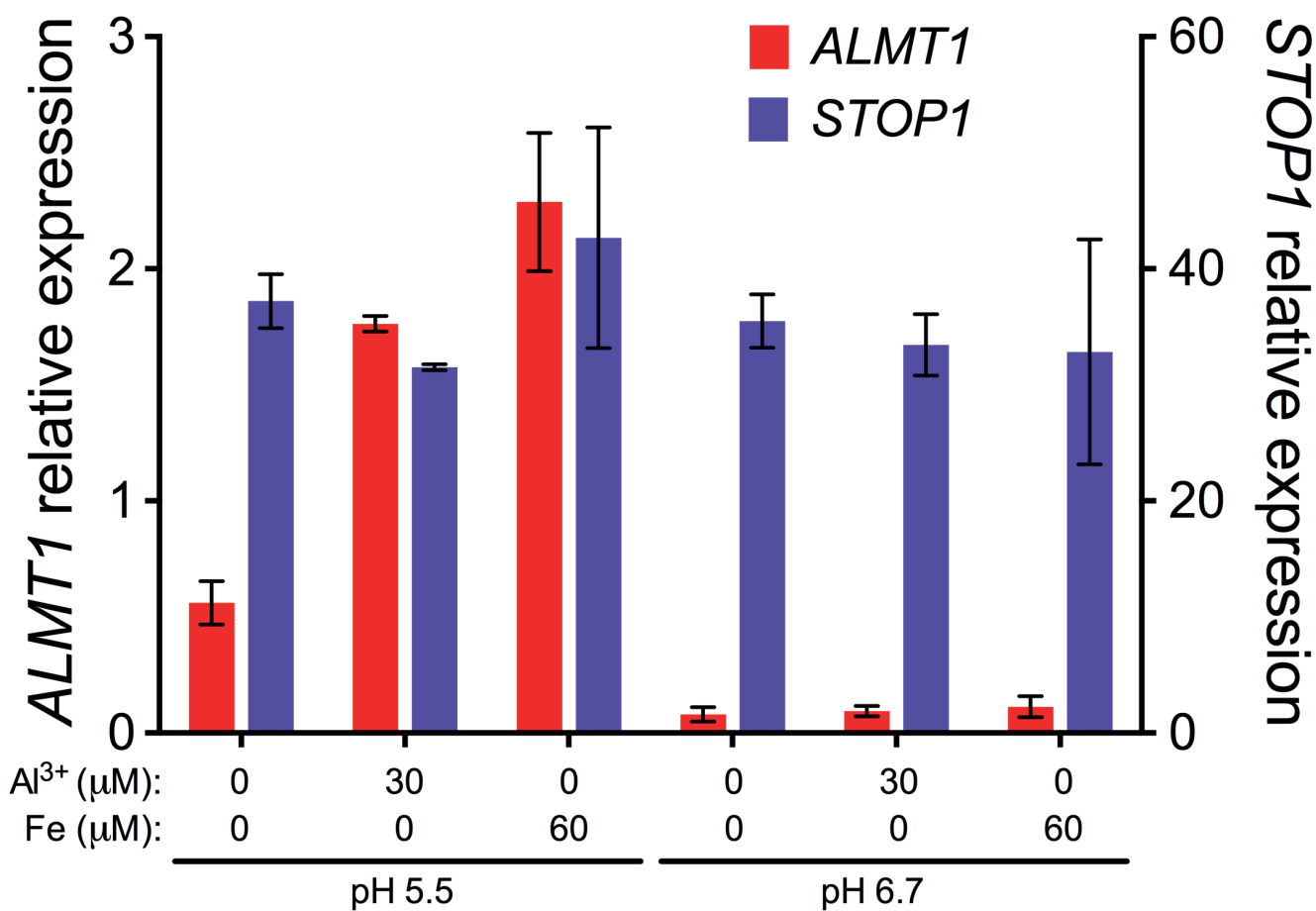
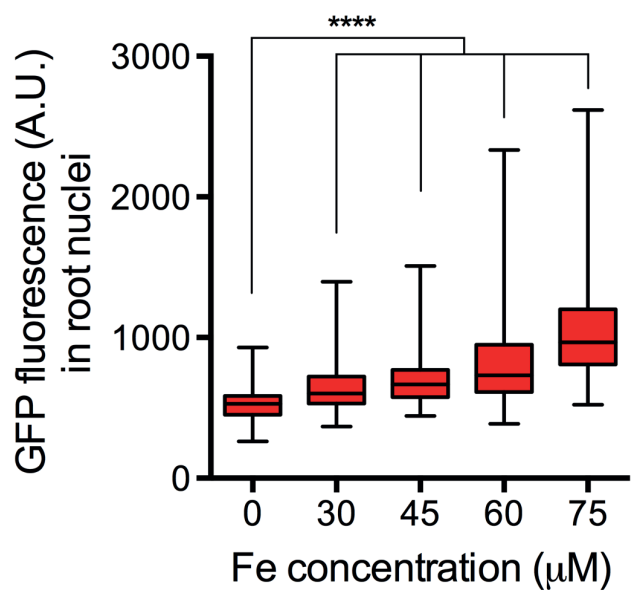


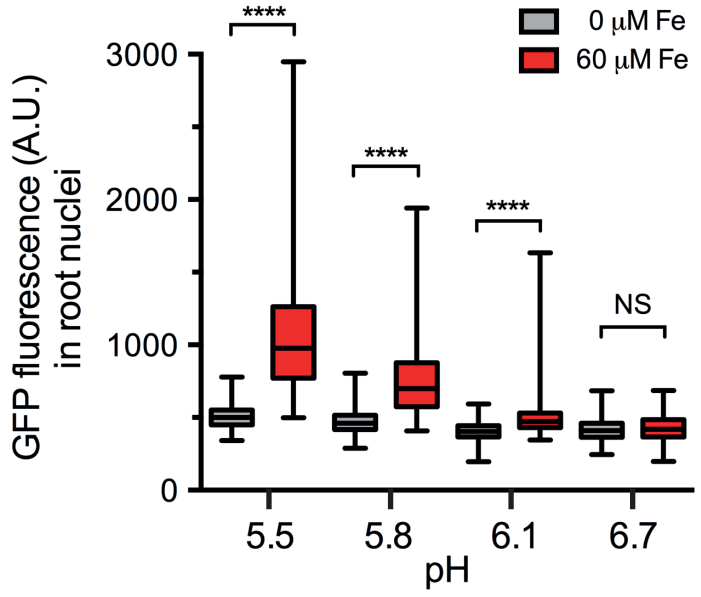
# Figure S4

1  
2  
3  
4  
5  
6  
7  
8  
9  
10  
11  
12  
13  
14  
15  
16  
17  
18  
19  
20  
21  
22  
23  
24  
25  
26  
27  
28  
29  
30  
31  
32  
33  
34  
35  
36  
37  
38  
39  
40  
41  
42  
43  
44  
45  
46  
47  
48  
49  
50  
51  
52  
53  
54  
55  
56  
57  
58  
59  
60

**a**



**c**



**b**

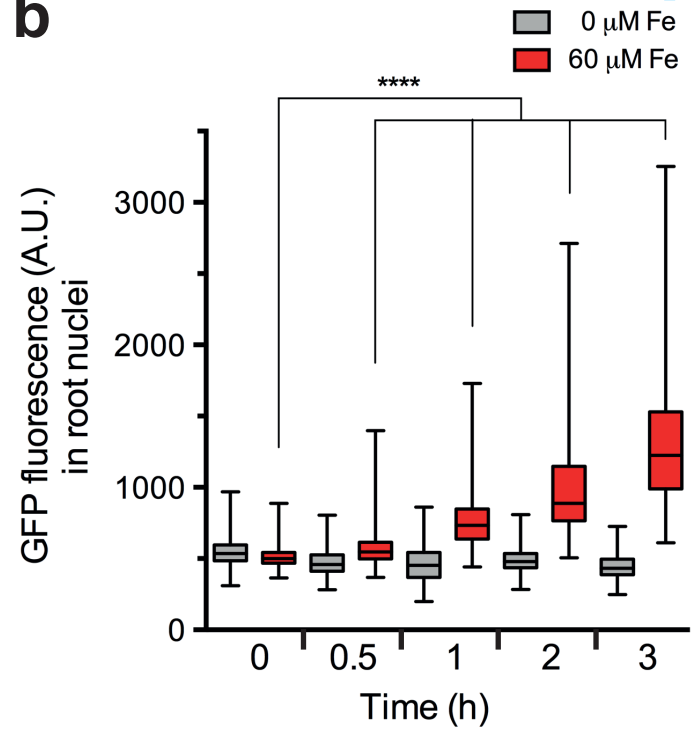


## Figure S5

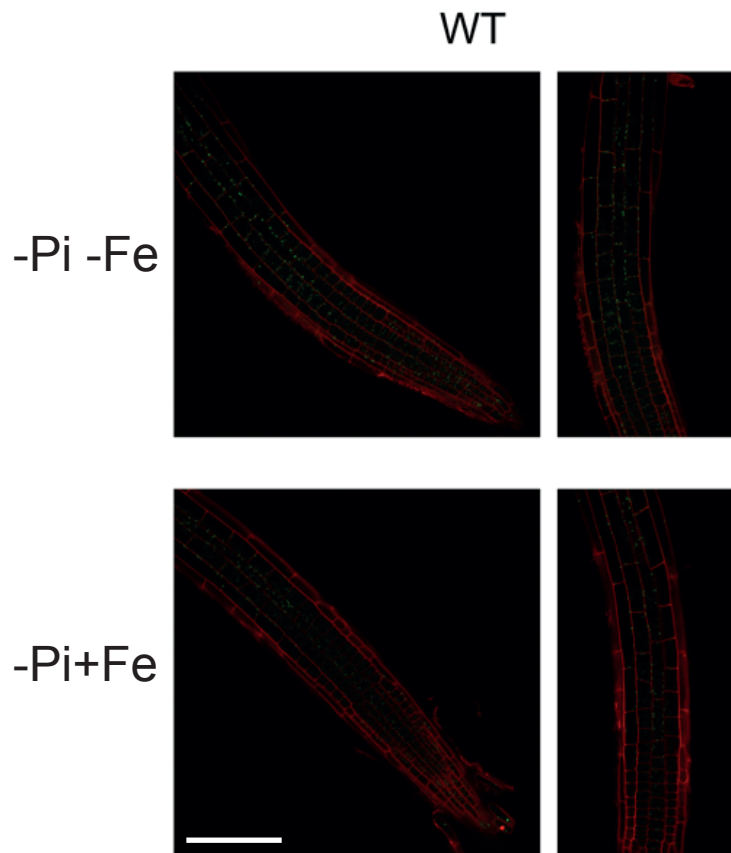
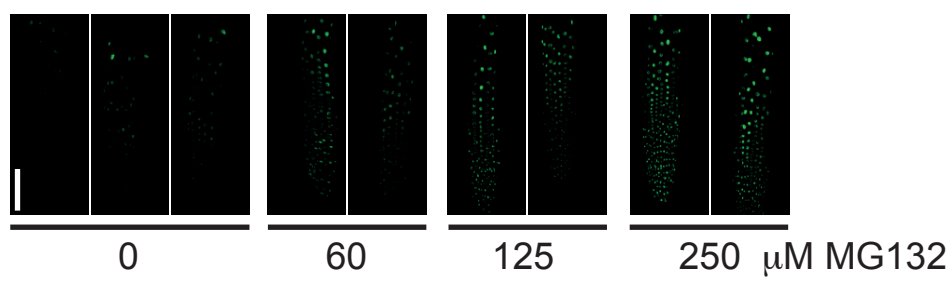


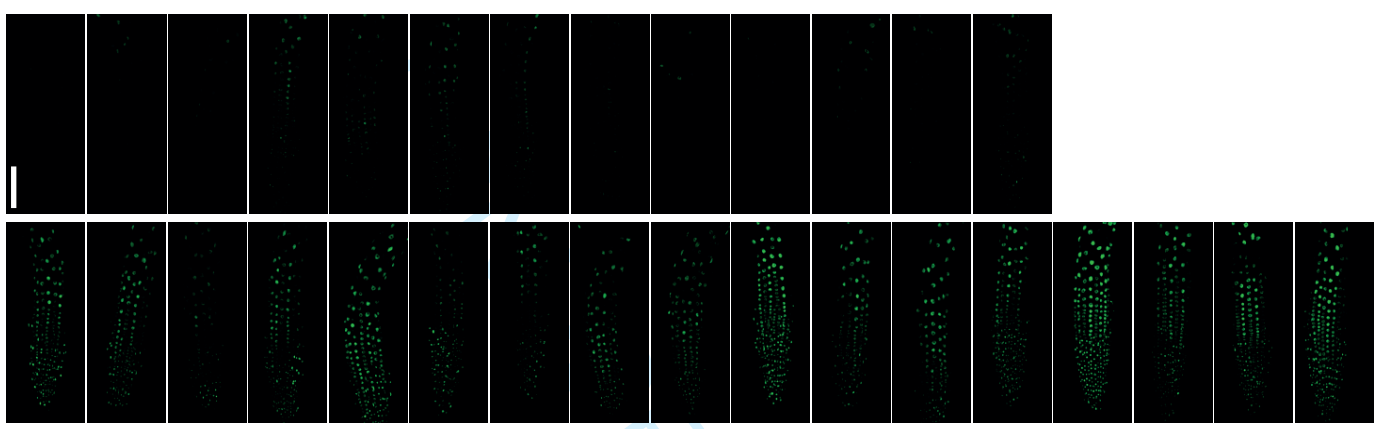
# Figure S6

1  
2  
3  
4  
5  
6  
7  
8  
9  
10  
11  
12  
13  
14  
15  
16  
17  
18  
19  
20  
21  
22  
23  
24  
25  
26  
27  
28  
29  
30  
31  
32  
33  
34  
35  
36  
37  
38  
39  
40  
41  
42  
43  
44  
45  
46  
47  
48  
49  
50  
51  
52  
53  
54  
55  
56  
57  
58  
59  
60

**a**



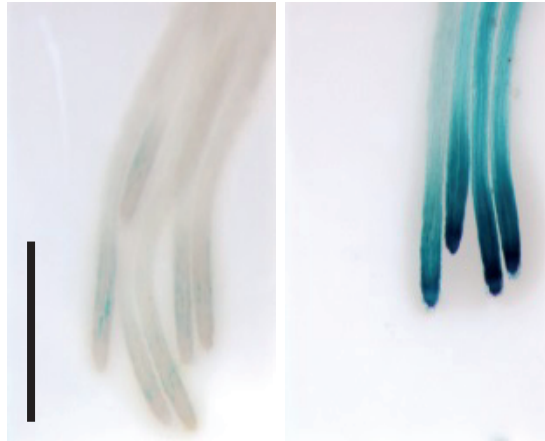
**b**



CONFIDENTIAL



## Figure S7



Al<sup>3+</sup> (μM):      0                      15

CONFIDENTIAL

## Figure S8

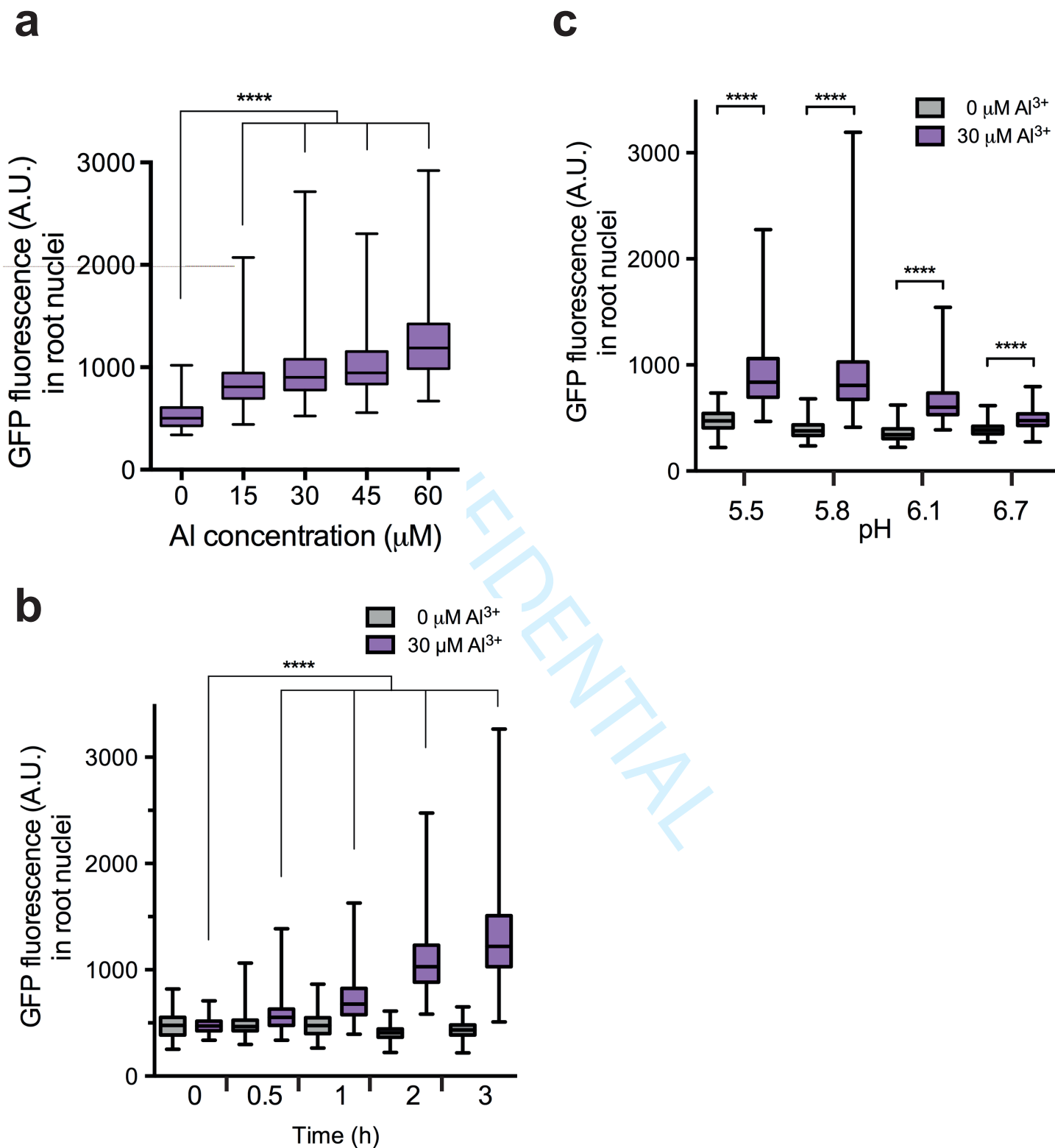


## Figure S9

